Electronic Transactions on Numerical Analysis.
Volume 44, pp. 250–270, 2015.
Copyright © 2015, Kent State University.
ISSN 1068–9613.

ETNA
Kent State University
http://etna.math.kent.edu

A CONVERGENT LINEAR FINITE ELEMENT SCHEME FOR THE MAXWELL-LANDAU-LIFSHITZ-GILBERT EQUATIONS*

L'. BAŇAS†, M. PAGE‡, AND D. PRAETORIUS‡

Abstract. We consider the lowest-order finite element discretization of the nonlinear system of Maxwell's and Landau-Lifshitz-Gilbert equations (MLLG). Two algorithms are proposed to numerically solve this problem, both of which only require the solution of at most two linear systems per time step. One of the algorithms is decoupled in the sense that it consists of the sequential computation of the magnetization and *afterwards* the magnetic and electric field. Under some mild assumptions on the effective field, we show that both algorithms converge towards weak solutions of the MLLG system. Numerical experiments for a micromagnetic benchmark problem demonstrate the performance of the proposed algorithms.

Key words. Maxwell-LLG, linear scheme, ferromagnetism, convergence

AMS subject classifications. 65N30, 65N50

1. Introduction.

The understanding of magnetization dynamics, especially on a microscale, is of utter relevance, for example in the development of magnetic sensors, recording heads, and magneto-resistive storage devices. In the literature, a well accepted model for micromagnetic phenomena is the Landau-Lifshitz-Gilbert equation (LLG); see (2.1a). This nonlinear partial differential equation describes the behaviour of the magnetization of some ferromagnetic body under the influence of a so-called effective field. Existence (and non-uniqueness) of weak solutions of LLG goes back to [5, 37]. Existence of weak solutions for MLLG was first shown in [18]. For a complete review of the analysis for LLG, we refer to [19, 22, 30] or the monographs [27, 34] and the references therein. As far as numerical simulation is concerned, convergent integrators can be found, e.g., in the works [13, 14] or [7], where the latter considers a weak integrator for the coupled MLLG system. From the viewpoint of numerical analysis, the integrator from [13] suffers from explicit time stepping, since this imposes a strong coupling of the time step size k and the spatial mesh size h. The integrators of [7, 14], on the other hand, rely on the implicit midpoint rule for time discretization, and unconditional stability and convergence is proved. In practice, a nonlinear system of equations has to be solved in each time step, and to that end, a fixed-point iteration is proposed in the works [7, 14]. This, however, again leads to a coupling of h and k, and thus destroys unconditional convergence. The problem can be reduced by using the Newton method for the midpoint scheme, which empirically allows for larger time steps; see [20] and also [8], where an efficient Newton-multigrid nonlinear solver has been proposed.

In [2], an unconditionally convergent projection-type integrator is proposed, which, despite the nonlinearity of LLG, only requires the solution of one linear system per time step. The effective field in this work, however, only covers microcrystalline exchange effects. In the subsequent works [3, 25, 26] the analysis for this integrator was extended to cover more general (linear) field contributions, where only the highest-order exchange contribution is treated implicitly, whereas the other contributions are treated explicitly. This allows reduction of the computational effort while still preserving unconditional convergence. Finally, in the very recent work [16], the authors could show unconditional convergence of this integrator, where

*Received June 29, 2013. Accepted February 2, 2015. Published online on May 7, 2015. Recommended by Axel Klawonn.

†Fakultät für Mathematik, Universität Bielefeld, Postfach 100 131, 33501 Bielefeld, Germany (banas@math.uni-bielefeld.de).

‡Institute for Analysis and Scientific Computing, Vienna University of Technology, Wiedner Hauptstraße 8-10, A-1040 Wien, Austria {Marcus.Page, Dirk.Praetorius}@tuwien.ac.at).

ETNA
Kent State University
http://etna.math.kent.edu

the effective field consists of some general energy contributions, which are only supposed to fulfill a certain set of properties. This particularly covers some nonlinear contributions, as well as certain multiscale problems. In addition, it is shown in [16] that errors arising due to approximate computation of field contributions like, e.g., the demagnetizing field, do not affect the unconditional convergence. In [4], the authors also investigate a higher-order extension of this algorithm which, however, requires implicit treatment of nonlocal contributions like the magnetostatic strayfield.

In our work, we extend the analysis of the aforementioned works and show that the integrator from [2] can be coupled with a weak formulation of the full Maxwell system (2.1b)–(2.1c). For the integration of this system, we propose two algorithms that only require the solution of one (Algorithm 4.1) resp. two linear systems (Algorithm 4.2) per time step while still guaranteeing unconditional convergence (Theorem 5.2). The contribution of the present work can be summarized as follows:

- We extend the linear integrator from [2, 25] to time-dependent contributions of the effective field by considering the full Maxwell equations instead of the magnetostatic simplification. This allows for more precise simulations (see, e.g., [23]) as well as the modeling of conducting ferromagnets (via $\sigma \neq 0$ in (2.1b)). The latter is unclear if one only considers the magnetostatic strayfield; cf. [32, Remark 1.4].
- Unlike [7], at most two linear systems per time step, instead of a coupled nonlinear system, need to be solved. Nevertheless, we still prove unconditional convergence.
- Unlike [7], we propose a fully decoupled scheme and show that the decoupling has no negative effect on the convergence behaviour. From a computational point of view, this is a major improvement over the current state of the art as it greatly simplifies preconditioning. Existing LLG or Maxwell solvers can be reused and only small modifications have to be done for the overall implementation.

Independently of the present work, [28] considered the coupling of LLG with the quasi-stationary eddy-current formulation of the Maxwell equations. There, however, only the coupled algorithm is proposed and analyzed. As far as the decoupling of the numerical integrator is concerned, the extended preprint [9] of the present work contained the first thorough numerical analysis and proof of unconditional convergence. Following [9], the work [28] derived a decoupled integrator for the eddy-current LLG system. Moreover, [10], analyzed the nonlinear coupling of LLG to the conservation of elastic momentum to model magnetostrictive effects and provided a decoupled time marching scheme. Finally, the recent work [1] analyzes the numerical integration of spin diffusion effects in spintronic micromagnetics.

Outline. The remainder of this paper is organized as follows: in Section 2, we recall the mathematical model for the full Maxwell-LLG system (MLLG) and recall the notion of a weak solution (Definition 2.1). In Section 3, we collect some notation and preliminaries, as well as the definition of the discrete ansatz spaces and their corresponding interpolation operators. In Section 4, we propose two algorithms (Algorithms 4.1 and 4.2) to approximate the MLLG system numerically. The large Section 5 is then devoted to our main convergence result (Theorem 5.2) and its proof. Finally, in Section 6, some numerical results conclude this work.

Notation. Throughout, $\boldsymbol{a} \cdot \boldsymbol{b}$ denotes the Euclidean scalar product of $\boldsymbol{a}, \boldsymbol{b}$ in $\mathbb{R}^d$ respectively $\mathbb{R}^{d\times d}$, and $|\boldsymbol{a}|$ denotes the corresponding Euclidean norm. Moreover, the $L^2(\Sigma)$-scalar product is denoted by $\langle \cdot, \cdot \rangle_\Sigma$. Finally, $A \lesssim B$ abbreviates $A \leq c\, B$ with some generic constant $c > 0$ which is clear from the context and, in particular, independent of the discretization parameters h and k.

2. Model problem.

We consider Maxwell-Landau-Lifshitz-Gilbert equations (MLLG), which describe the evolution of the magnetization of a ferromagnetic body that occupies

ETNA
Kent State University
http://etna.math.kent.edu

the domain $\omega \Subset \Omega \subseteq \mathbb{R}^3$. For a given damping parameter $\alpha > 0$, the magnetization $\mathbf{m}\colon (0,T)\times\omega \to \mathbb{S}^2$ and the electric and magnetic fields $\mathbf{E},\mathbf{H}\colon (0,T)\times\Omega\to\mathbb{R}^3$ satisfy the MLLG system

$$\mathbf{m}_t - \alpha\mathbf{m}\times\mathbf{m}_t = -\mathbf{m}\times\mathbf{H}_{\text{eff}} \qquad \text{in } \omega_T := (0,T)\times\omega, \tag{2.1a}$$

$$\varepsilon_0\mathbf{E}_t - \nabla\times\mathbf{H} + \sigma\chi_\omega\mathbf{E} = -\mathbf{J} \qquad \text{in } \Omega_T := (0,T)\times\Omega, \tag{2.1b}$$

$$\mu_0\mathbf{H}_t + \nabla\times\mathbf{E} = -\mu_0\chi_\omega\,\mathbf{m}_t \qquad \text{in } \Omega_T, \tag{2.1c}$$

where the effective field $\mathbf{H}_{\text{eff}}$ consists of $\mathbf{H}_{\text{eff}} = C_e\Delta\mathbf{m} + \mathbf{H} + \pi(\mathbf{m})$ for some general energy contribution π which is assumed to fulfill a certain set of properties; see (5.3)–(5.4). This is in analogy to [16]. We stress that, with the techniques from [16], an approximation π_h of π can be included into the analysis as well. We emphasize that throughout this work, the case $\mathbf{H}_{\text{eff}} = C_e\Delta\mathbf{m} + \mathbf{H} + C_aD\Phi(\mathbf{m}) + \mathbf{H}_{ext}$ is particularly covered. Here, $\Phi(\cdot)$ denotes the crystalline anisotropy density and $\mathbf{H}_{ext}$ is a given applied field. The constants $\varepsilon_0,\mu_0 \geq 0$ denote the electric and magnetic permeability of free space, respectively, and the constant $\sigma \geq 0$ stands for the conductivity of the ferromagnetic domain ω. The field $\mathbf{J}\colon \Omega_T \to \mathbb{R}^3$ describes an applied current density and $\chi_\omega\colon \Omega\to\{0,1\}$ is the characteristic function of ω. As is usually done for simplicity, we assume $\Omega\subset\mathbb{R}^3$ to be bounded with perfectly conducting outer surface $\partial\Omega$ into which the ferromagnet $\omega \Subset \Omega$ is embedded, and $\Omega\backslash\overline{\omega}$ is assumed to be vacuum. In addition, the MLLG system (2.1) is supplemented by initial conditions

$$\mathbf{m}(0,\cdot) = \mathbf{m}^0 \quad \text{in } \omega \qquad \text{and} \qquad \mathbf{E}(0,\cdot) = \mathbf{E}^0, \quad \mathbf{H}(0,\cdot) = \mathbf{H}^0 \quad \text{in } \Omega \tag{2.1d}$$

as well as boundary conditions

$$\partial_{\mathbf{n}}\mathbf{m} = 0 \quad \text{on } \partial\omega_T, \qquad \mathbf{E}\times\mathbf{n} = 0 \quad \text{on } \partial\Omega_T, \tag{2.1e}$$

where $\partial\omega_T$ and $\partial\Omega_T$ denote the spatial boundaries and $\mathbf{n}$ is the respective outer normal vector. Note that the side constraint $|\mathbf{m}| = 1$ a.e. in ω_T does not need to be enforced explicitly, but follows from $|\mathbf{m}^0| = 1$ a.e. in ω and $\partial_t|\mathbf{m}|^2 = 2\mathbf{m}\cdot\mathbf{m}_t = 0$ in ω_T, which is a consequence of (2.1a). This behaviour should also be reflected by the numerical integrator. In analogy to [7, 18], we assume the given data to satisfy

$$\mathbf{m}^0 \in H^1(\omega,\mathbb{S}^2), \qquad \mathbf{H}^0,\mathbf{E}^0 \in \mathbf{L}^2(\Omega,\mathbb{R}^3), \qquad \mathbf{J}\in\mathbf{L}^2(\Omega_T,\mathbb{R}^3) \tag{2.1f}$$

as well as

$$\operatorname{div}(\mathbf{H}^0 + \chi_\omega\mathbf{m}^0) = 0 \quad \text{in } \Omega, \qquad (\mathbf{H}^0 + \chi_\omega\mathbf{m}^0)\cdot\mathbf{n} = 0 \quad \text{on } \partial\Omega. \tag{2.1g}$$

With the space

$$\mathbf{H}_0(\mathbf{curl},\Omega) := \big\{\varphi\in\mathbf{L}^2(\Omega)\ :\ \nabla\times\varphi\in\mathbf{L}^2(\Omega), \varphi\times\mathbf{n} = 0 \text{ on } \Gamma\big\},$$

we now recall the notion of a weak solution of (2.1a)–(2.1c) from [18].

DEFINITION 2.1. *Given (2.1f)–(2.1g), the tupel $(\mathbf{m},\mathbf{E},\mathbf{H})$ is called a weak solution of MLLG (2.1) if,*

(i) $\mathbf{m}\in\mathbf{H}^1(\omega_T)$ with $|\mathbf{m}| = 1$ almost everywhere in ω_T and $(\mathbf{E},\mathbf{H})\in\mathbf{L}^2(\Omega_T)$;

(ii) for all $\boldsymbol{\varphi}\in C^\infty(\omega_T)$ and $\boldsymbol{\zeta}\in C_c^\infty\big([0,T); C^\infty(\Omega)\cap\mathbf{H}^0(\mathbf{curl},\Omega)\big)$, we have

$$\begin{aligned}\int_{\omega_T}\mathbf{m}_t\cdot\boldsymbol{\varphi} - \alpha\int_{\omega_T}(\mathbf{m}\times\mathbf{m}_t)\cdot\boldsymbol{\varphi}\\ = -C_e\int_{\omega_T}(\nabla\mathbf{m}\times\mathbf{m})\cdot\nabla\boldsymbol{\varphi} + \int_{\omega_T}(\mathbf{H}\times\mathbf{m})\cdot\boldsymbol{\varphi} + \int_{\omega_T}(\pi(\mathbf{m})\times\mathbf{m})\cdot\boldsymbol{\varphi},\end{aligned} \tag{2.2}$$

ETNA
Kent State University
http://etna.math.kent.edu

$$
\begin{aligned}
&-\varepsilon_0 \int_{\Omega_T} \mathbf{E}\cdot\boldsymbol{\zeta}_t - \int_{\Omega_T} \mathbf{H}\cdot(\nabla\times\boldsymbol{\zeta}) + \sigma\int_{\omega_T}\mathbf{E}\cdot\boldsymbol{\zeta}\\
&\qquad = -\int_{\Omega_T}\mathbf{J}\cdot\boldsymbol{\zeta} + \varepsilon_0\int_\Omega \mathbf{E}^0\cdot\boldsymbol{\zeta}(0,\cdot),
\end{aligned}
\tag{2.3}
$$

$$
-\mu_0\int_{\Omega_T}\mathbf{H}\cdot\boldsymbol{\zeta}_t + \int_{\Omega_T}\mathbf{E}\cdot(\nabla\times\boldsymbol{\zeta}) = -\mu_0\int_{\omega_T}\mathbf{m}_t\cdot\boldsymbol{\zeta} + \mu_0\int_\Omega \mathbf{H}^0\cdot\boldsymbol{\zeta}(0,\cdot);
\tag{2.4}
$$

(iii) there holds $\mathbf{m}(0,\cdot)=\mathbf{m}^0$ *in the sense of traces;*
(iv) for almost all $t'\in(0,T)$*, we have bounded energy*

$$
\|\nabla\mathbf{m}(t')\|^2_{\mathbf{L}^2(\omega)} + \|\mathbf{m}_t\|^2_{\mathbf{L}^2(\omega_{t'})} + \|\mathbf{H}(t')\|^2_{\mathbf{L}^2(\Omega)} + \|\mathbf{E}(t')\|^2_{\mathbf{L}^2(\Omega)} \le C,
\tag{2.5}
$$

where $C>0$ *is independent of* t.

Existence of weak solutions was first shown in [18]. We note, however, that our analysis is constructive in the sense that it also proves existence.

REMARK 2.2. Under additional assumptions on the general contribution $\pi(\cdot)$, namely that $\pi(\cdot)$ is self-adjoint with $\|\pi(\mathbf{n})\|_{\mathbf{L}^4(\omega)} \le C$ for all $\mathbf{n}\in\mathbf{L}^2(\omega)$ with $|\mathbf{n}|\le 1$ almost everywhere, the energy estimate (2.5) can be improved. The same techniques as in [16, Appendix A] then show for almost all $t'\in(0,T)$ and $\varepsilon>0$ that

$$
\begin{aligned}
&\mathcal{E}(\mathbf{m},\mathbf{H},\mathbf{E})(t') + 2(\alpha-\varepsilon)\mu_0\|\mathbf{m}_t\|^2_{\mathbf{L}^2(\omega_{t'})} + 2\sigma\|\mathbf{E}\|^2_{\mathbf{L}^2(\omega_{t'})}\\
&\qquad \le \mathcal{E}(\mathbf{m},\mathbf{H},\mathbf{E})(0) - \int_0^{t'}\langle\mathbf{J},\mathbf{E}\rangle_\Omega,
\end{aligned}
$$

where

$$
\mathcal{E}(\mathbf{m},\mathbf{H},\mathbf{E}) := \mu_0 C_e\|\nabla\mathbf{m}\|^2_{\mathbf{L}^2(\omega)} + \mu_0\|\mathbf{H}\|^2_{\mathbf{L}^2(\Omega)} + \varepsilon_0\|\mathbf{E}\|^2_{\mathbf{L}^2(\omega)} - \mu_0\langle\pi(\mathbf{m}),\mathbf{m}\rangle_\omega.
$$

This is in analogy to [7]. In particular, the above assumptions are fulfilled in case of vanishing applied field $\mathbf{H}_{ext}\equiv 0$ and if $\pi(\cdot)$ denotes the uniaxial anisotropy density.

3. Preliminaries. For time discretization, we impose a uniform partition of the time interval $[0,T]$, $0=t_0<t_1<\ldots<t_N=T$. The time step size is denoted by $k=k_j:=t_{j+1}-t_j$ for $j=0,\ldots,N-1$. For each (discrete) function $\boldsymbol{\varphi},\boldsymbol{\varphi}^j:=\boldsymbol{\varphi}(t_j)$ denotes the evaluation at time t_j. Furthermore, we write $d_t\boldsymbol{\varphi}^{j+1}:=(\boldsymbol{\varphi}^{j+1}-\boldsymbol{\varphi}^j)/k$ for $j\ge 1$, and $\boldsymbol{\varphi}^{j+1/2}:=(\boldsymbol{\varphi}^{j+1}+\boldsymbol{\varphi}^j)/2$ for $j\ge 0$ and a sequence $\{\boldsymbol{\varphi}^j\}_{j\ge 0}$.

For the spatial discretization, let $\mathcal{T}_h^\Omega$ be a regular triangulation of the polyhedral bounded Lipschitz domain $\Omega\subset\mathbb{R}^3$ into compact and non-degenerate tetrahedra. By $\mathcal{T}_h$, we denote its restriction to $\omega\Subset\Omega$, where we assume that ω is resolved, i.e.,

$$
\mathcal{T}_h = \mathcal{T}_h^\Omega|_\omega = \big\{T\in\mathcal{T}_h^\Omega : T\cap\omega\neq\emptyset\big\} \quad\text{and}\quad \overline{\omega} = \bigcup_{T\in\mathcal{T}_h} T.
$$

By $\mathcal{S}^1(\mathcal{T}_h)$ we denote the standard $\mathcal{P}^1$-FEM space of globally continuous and piecewise affine functions from ω to $\mathbb{R}^3$

$$
\mathcal{S}^1(\mathcal{T}_h) := \{\boldsymbol{\phi}_h\in C(\overline{\omega},\mathbb{R}^3) : \boldsymbol{\phi}_h|_K\in\mathcal{P}_1(K)\text{ for all } K\in\mathcal{T}_h\}.
$$

ETNA
Kent State University
http://etna.math.kent.edu

By $\mathcal{I}_h\colon C(\Omega) \to \mathcal{S}^1(\mathcal{T}_h)$, we denote the nodal interpolation operator onto this space. Now, let the set of nodes of the triangulation $\mathcal{T}_h$ be denoted by $\mathcal{N}_h$. For discretization of the magnetization $\mathbf{m}$ in the LLG equation (2.1a), we define the set of admissible discrete magnetizations by

$$\mathcal{M}_h := \{\boldsymbol{\phi}_h \in \mathcal{S}^1(\mathcal{T}_h) : |\boldsymbol{\phi}_h(\mathbf{z})| = 1 \text{ for all } \mathbf{z} \in \mathcal{N}_h\}.$$

Due to the modulus constraint $|\mathbf{m}(t)| = 1$, and therefore $\mathbf{m}_t \cdot \mathbf{m} = 0$ almost everywhere in ω_T, we discretize the time derivative $\mathbf{v}(t_j) := \mathbf{m}_t(t_j)$ in the discrete tangent space which is defined by

$$\mathcal{K}_{\boldsymbol{\phi}_h} := \{\boldsymbol{\psi}_h \in \mathcal{S}^1(\mathcal{T}_h|_\omega) : \boldsymbol{\psi}_h(\mathbf{z}) \cdot \boldsymbol{\phi}_h(\mathbf{z}) = 0 \text{ for all } \mathbf{z} \in \mathcal{N}_h\}$$

for any $\boldsymbol{\phi}_h \in \mathcal{M}_h$.

To discretize the Maxwell equations (2.1b)–(2.1c), we use conforming ansatz spaces $\mathcal{X}_h \subset \mathbf{H}^0(\mathbf{curl}; \Omega)$, $\mathcal{Y}_h \subset \mathbf{L}^2(\Omega)$ subordinate to $\mathcal{T}_h^\Omega$ which additionally fulfill $\nabla \times \mathcal{X}_h \subset \mathcal{Y}_h$. In analogy to [7], we choose first-order edge elements

$$\mathcal{X}_h := \{\boldsymbol{\varphi}_h \in \mathbf{H}^0(\mathbf{curl}; \Omega) : \boldsymbol{\varphi}_h|_K \in \mathcal{P}_1(K) \text{ for all } K \in \mathcal{T}_h^\Omega\}$$

and piecewise constants

$$\mathcal{Y}_h := \{\boldsymbol{\zeta}_h \in \mathbf{L}^2(\Omega) : \boldsymbol{\zeta}_h|_K \in \mathcal{P}_0(K) \text{ for all } K \in \mathcal{T}_h^\Omega\};$$

cf. [31, Chapter 8.5]. Associated with $\mathcal{X}_h$, let $\mathcal{I}_{\mathcal{X}_h}\colon \mathbf{H}^2(\Omega) \to \mathcal{X}_h$ denote the corresponding nodal FEM interpolator. Moreover, let

$$\mathcal{I}_{\mathcal{Y}_h}\colon \mathbf{L}^2(\Omega) \to \mathcal{Y}_h$$

denote the $\mathbf{L}^2$-orthogonal projection characterized by

$$\langle \boldsymbol{\zeta} - \mathcal{I}_{\mathcal{Y}_h}\boldsymbol{\zeta}, \mathbf{y}_h\rangle_\Omega = 0 \qquad \text{for all } \boldsymbol{\zeta} \in \mathbf{L}^2(\Omega) \text{ and } \mathbf{y}_h \in \mathcal{Y}_h.$$

By standard estimates (see, e.g., [15, 31]) one derives the approximation properties

$$\|\boldsymbol{\varphi} - \mathcal{I}_{\mathcal{X}_h}\boldsymbol{\varphi}\|_{\mathbf{L}^2(\Omega)} + h\|\nabla \times (\boldsymbol{\varphi} - \mathcal{I}_{\mathcal{X}_h}\boldsymbol{\varphi})\|_{\mathbf{L}^2(\Omega)} \le C\, h^2 \|\nabla^2 \boldsymbol{\varphi}\|_{\mathbf{L}^2(\Omega)}, \tag{3.1}$$

$$\|\boldsymbol{\zeta} - \mathcal{I}_{\mathcal{Y}_h}\boldsymbol{\zeta}\|_{\mathbf{L}^2(\Omega)} \le C\, h \|\boldsymbol{\zeta}\|_{\mathbf{H}^1(\Omega)}, \tag{3.2}$$

for all $\boldsymbol{\varphi} \in \mathbf{H}^2(\Omega)$ and $\boldsymbol{\zeta} \in \mathbf{H}^1(\Omega)$.

4. Numerical algorithms. We recall that the LLG equation (2.1a) can equivalently be stated as

$$\alpha \mathbf{m}_t + \mathbf{m} \times \mathbf{m}_t = \mathbf{H}_{\text{eff}} - (\mathbf{m} \cdot \mathbf{H}_{\text{eff}})\mathbf{m}$$

under the constraint $|\mathbf{m}| = 1$ almost everywhere in Ω_T. This formulation will now be used to construct the numerical schemes. Following the approaches of Alouges et al. [2, 3] and Bruckner et al. from [16], we propose two algorithms for the numerical integration of MLLG, where the first one follows the lines of [7].

ETNA
Kent State University
http://etna.math.kent.edu

4.1. MLLG integrators. For ease of presentation, we assume that the applied field $\mathbf{J}$ is continuous in time, i.e., $\mathbf{J} \in C\big([0,T];\mathbf{L}^2(\Omega)\big)$ so that $\mathbf{J}^j := \mathbf{J}(t_j)$ is meaningful. We emphasize, however, that this is not necessary for our convergence analysis.

ALGORITHM 4.1. Input: Initial data $\mathbf{m}^0$, $\mathbf{E}^0$, and $\mathbf{H}^0$, parameter $\theta \in [0,1]$, counter $j = 0$. For all $j = 0, \dots, N-1$ iterate:

(i) Compute the unique solution $(\mathbf{v}_h^j, \mathbf{E}_h^{j+1}, \mathbf{H}_h^{j+1}) \in (\mathcal{K}_{\mathbf{m}_h^j}, \mathcal{X}_h, \mathcal{Y}_h)$ such that for all $(\boldsymbol{\phi}_h, \boldsymbol{\psi}_h, \boldsymbol{\zeta}_h) \in \mathcal{K}_{\mathbf{m}_h^j} \times \mathcal{X}_h \times \mathcal{Y}_h$ it holds that

$$\alpha\langle \mathbf{v}_h^j, \boldsymbol{\phi}_h\rangle_\omega + \langle \mathbf{m}_h^j \times \mathbf{v}_h^j, \boldsymbol{\phi}_h\rangle_\omega = -C_e\langle \nabla(\mathbf{m}_h^j + \theta k \mathbf{v}_h^j), \nabla\boldsymbol{\phi}_h\rangle_\omega + \langle \mathbf{H}_h^{j+1/2}, \boldsymbol{\phi}_h\rangle_\omega + \langle \pi(\mathbf{m}_h^j), \boldsymbol{\phi}_h\rangle_\omega, \tag{4.1a}$$

$$\varepsilon_0\langle d_t\mathbf{E}_h^{j+1}, \boldsymbol{\psi}_h\rangle_\Omega - \langle \mathbf{H}_h^{j+1/2}, \nabla\times\boldsymbol{\psi}_h\rangle_\Omega + \sigma\langle \chi_\omega \mathbf{E}_h^{j+1/2}, \boldsymbol{\psi}_h\rangle_\Omega = -\langle \mathbf{J}^{j+1/2}, \boldsymbol{\psi}_h\rangle_\Omega, \tag{4.1b}$$

$$\mu_0\langle d_t\mathbf{H}_h^{j+1}, \boldsymbol{\zeta}_h\rangle_\Omega + \langle \nabla\times\mathbf{E}_h^{j+1/2}, \boldsymbol{\zeta}_h\rangle_\Omega = -\mu_0\langle \mathbf{v}_h^j, \boldsymbol{\zeta}_h\rangle_\omega. \tag{4.1c}$$

(ii) Define $\mathbf{m}_h^{j+1} \in \mathcal{M}_h$ nodewise by $\mathbf{m}_h^{j+1}(\mathbf{z}) = \dfrac{\mathbf{m}_h^j(\mathbf{z}) + k\mathbf{v}_h^j(\mathbf{z})}{|\mathbf{m}_h^j(\mathbf{z}) + k\mathbf{v}_h^j(\mathbf{z})|}$ for all $\mathbf{z} \in \mathcal{N}_h$.

For the sake of computational and implementational ease, LLG and Maxwell equations can be decoupled which leads to only two linear systems per time step. This modification is explicitly stated in the second algorithm.

ALGORITHM 4.2. Input: Initial data $\mathbf{m}^0$, $\mathbf{E}^0$, and $\mathbf{H}^0$, parameter $\theta \in [0,1]$, counter $j = 0$. For all $j = 0, \dots, N-1$ iterate:

(i) Compute the unique solution $\mathbf{v}_h^j \in \mathcal{K}_{\mathbf{m}_h^j}$ such that for all $\boldsymbol{\phi}_h \in \mathcal{K}_{\mathbf{m}_h^j}$ it holds that

$$\alpha\langle \mathbf{v}_h^j, \boldsymbol{\phi}_h\rangle_\omega + \langle \mathbf{m}_h^j \times \mathbf{v}_h^j, \boldsymbol{\phi}_h\rangle_\omega = -C_e\langle \nabla(\mathbf{m}_h^j + \theta k \mathbf{v}_h^j), \nabla\boldsymbol{\phi}_h\rangle_\omega + \langle \mathbf{H}_h^j, \boldsymbol{\phi}_h\rangle_\omega + \langle \pi(\mathbf{m}_h^j), \boldsymbol{\phi}_h\rangle_\omega. \tag{4.2a}$$

(ii) Compute the unique solution $(\mathbf{E}_h^{j+1}, \mathbf{H}_h^{j+1}) \in (\mathcal{X}_h, \mathcal{Y}_h)$ such that for all $(\boldsymbol{\psi}_h, \boldsymbol{\zeta}_h) \in \mathcal{X}_h \times \mathcal{Y}_h$ it holds that

$$\varepsilon_0\langle d_t\mathbf{E}_h^{j+1}, \boldsymbol{\psi}_h\rangle_\Omega - \langle \mathbf{H}_h^{j+1}, \nabla\times\boldsymbol{\psi}_h\rangle_\Omega + \sigma\langle \chi_\omega \mathbf{E}_h^{j+1}, \boldsymbol{\psi}_h\rangle_\Omega = -\langle \mathbf{J}^j, \boldsymbol{\psi}_h\rangle_\Omega, \tag{4.2b}$$

$$\mu_0\langle d_t\mathbf{H}_h^{j+1}, \boldsymbol{\zeta}_h\rangle_\Omega + \langle \nabla\times\mathbf{E}_h^{j+1}, \boldsymbol{\zeta}_h\rangle_\Omega = -\mu_0\langle \mathbf{v}_h^j, \boldsymbol{\zeta}_h\rangle_\omega. \tag{4.2c}$$

(iii) Define $\mathbf{m}_h^{j+1} \in \mathcal{M}_h$ nodewise by $\mathbf{m}_h^{j+1}(\mathbf{z}) = \dfrac{\mathbf{m}_h^j(\mathbf{z}) + k\mathbf{v}_h^j(\mathbf{z})}{|\mathbf{m}_h^j(\mathbf{z}) + k\mathbf{v}_h^j(\mathbf{z})|}$ for all $\mathbf{z} \in \mathcal{N}_h$.

4.2. Unique solvability. In this brief section, we show that the two above algorithms are indeed well defined and admit unique solutions in each step of the iterative loop. We start with Algorithm 4.1.

LEMMA 4.3. *Algorithm 4.1 is well defined in the sense that in each step $j = 0, \dots, N-1$ of the loop, there exist unique solutions $(\mathbf{m}_h^{j+1}, \mathbf{v}_h^j, \mathbf{E}_h^{j+1}, \mathbf{H}_h^{j+1})$.*

ETNA
Kent State University
http://etna.math.kent.edu

Proof. We multiply the first equation of (4.1) by μ_0 and the second and third equation by some free parameter $C_1 > 0$ to define the bilinear form $a^j(\cdot,\cdot)$ on $(\mathcal{K}_{\mathbf{m}_h^j}, \mathcal{X}_h, \mathcal{Y}_h)$ by

$$\begin{aligned}
&a^j\big((\boldsymbol{\Phi},\boldsymbol{\Psi},\boldsymbol{\Theta}),(\boldsymbol{\phi},\boldsymbol{\psi},\boldsymbol{\zeta})\big)\\
&\quad:= \alpha\mu_0\,\langle\boldsymbol{\Phi},\boldsymbol{\phi}\rangle_\omega + \mu_0\,\langle\mathbf{m}_h^j\times\boldsymbol{\Phi},\boldsymbol{\phi}\rangle_\omega + \mu_0 C_e\theta k\,\langle\nabla\boldsymbol{\Phi},\nabla\boldsymbol{\phi}\rangle_\omega - \frac{\mu_0}{2}\langle\boldsymbol{\Theta},\boldsymbol{\zeta}\rangle_\Omega\\
&\qquad+ \frac{C_1\varepsilon_0}{k}\langle\boldsymbol{\Psi},\boldsymbol{\psi}\rangle_\Omega - \frac{C_1}{2}\langle\boldsymbol{\Theta},\nabla\times\boldsymbol{\psi}\rangle_\Omega + \frac{C_1\sigma}{2}\langle\boldsymbol{\Psi},\boldsymbol{\psi}\rangle_\omega\\
&\qquad+ \frac{C_1\mu_0}{k}\langle\boldsymbol{\Theta},\boldsymbol{\zeta}\rangle_\Omega + \frac{C_1}{2}\langle\nabla\times\boldsymbol{\Psi},\boldsymbol{\zeta}\rangle_\Omega + C_1\mu_0\,\langle\boldsymbol{\Phi},\boldsymbol{\zeta}\rangle_\omega
\end{aligned}$$

and the linear functional $L^j(\cdot)$ on $(\mathcal{K}_{\mathbf{m}_h^j}, \mathcal{X}_h, \mathcal{Y}_h)$ by

$$\begin{aligned}
L^j\big((\boldsymbol{\phi},\boldsymbol{\psi},\boldsymbol{\zeta})\big) &:= -\mu_0 C_e\,\langle\nabla\mathbf{m}_h^j,\nabla\boldsymbol{\phi}\rangle_\omega + \frac{\mu_0}{2}\langle\mathbf{H}_h^j,\boldsymbol{\phi}\rangle_\omega + \mu_0\,\langle\pi(\mathbf{m}_h^j),\boldsymbol{\phi}\rangle_\omega\\
&\quad- C_1\langle\mathbf{J}^{j+1/2},\boldsymbol{\psi}\rangle_\Omega + \frac{C_1\varepsilon_0}{k}\langle\mathbf{E}_h^j,\boldsymbol{\psi}\rangle_\Omega + \frac{C_1}{2}\langle\mathbf{H}_h^j,\nabla\times\boldsymbol{\psi}\rangle_\Omega - \frac{C_1\sigma}{2}\langle\mathbf{E}_h^j,\boldsymbol{\psi}\rangle_\omega\\
&\quad+ \frac{C_1\mu_0}{k}\langle\mathbf{H}_h^j,\boldsymbol{\zeta}\rangle_\Omega - \frac{C_1}{2}\langle\nabla\times\mathbf{E}_h^j,\boldsymbol{\zeta}\rangle_\Omega.
\end{aligned}$$

To ease the readability, the respective first lines of these definitions stem from (4.1a), the second from (4.1b), and the third from (4.1c). Clearly, (4.1) is equivalent to

$$a^j\big((\mathbf{v}_h^j,\mathbf{E}_h^{j+1},\mathbf{H}_h^{j+1}),(\boldsymbol{\phi}_h,\boldsymbol{\psi}_h,\boldsymbol{\zeta}_h)\big) = L\big((\boldsymbol{\phi}_h,\boldsymbol{\psi}_h,\boldsymbol{\zeta}_h)\big)$$

for all $(\boldsymbol{\phi}_h,\boldsymbol{\psi}_h,\boldsymbol{\zeta}_h) \in \mathcal{K}_{\mathbf{m}_h^j}\times\mathcal{X}_h\times\mathcal{Y}_h$. Next, we aim to show that the bilinear form $a^j(\cdot,\cdot)$ is positive definite on $\mathcal{K}_{\mathbf{m}_h^j}\times\mathcal{X}_h\times\mathcal{Y}_h$. Usage of the Hölder inequality reveals that for all $(\boldsymbol{\varphi},\boldsymbol{\psi},\boldsymbol{\zeta}) \in \mathcal{K}_{\mathbf{m}_h^j}\times\mathcal{X}_h\times\mathcal{Y}_h$ it holds that

$$\begin{aligned}
&a^j\big((\boldsymbol{\phi},\boldsymbol{\psi},\boldsymbol{\zeta}),(\boldsymbol{\phi},\boldsymbol{\psi},\boldsymbol{\zeta})\big)\\
&\quad= \alpha\mu_0\langle\boldsymbol{\phi},\boldsymbol{\phi}\rangle_\omega + \mu_0\langle\mathbf{m}_h^j\times\boldsymbol{\phi},\boldsymbol{\phi}\rangle_\omega + \mu_0 C_e\theta k\,\langle\nabla\boldsymbol{\phi},\nabla\boldsymbol{\phi}\rangle_\omega - \frac{\mu_0}{2}\,\langle\boldsymbol{\phi},\boldsymbol{\zeta}\rangle_\omega\\
&\qquad+ \frac{C_1\varepsilon_0}{k}\langle\boldsymbol{\psi},\boldsymbol{\psi}\rangle_\Omega - \frac{C_1}{2}\langle\boldsymbol{\zeta},\nabla\times\boldsymbol{\psi}\rangle_\Omega + \frac{C_1\sigma}{2}\langle\boldsymbol{\psi},\boldsymbol{\psi}\rangle_\omega\\
&\qquad+ \frac{C_1\mu_0}{k}\langle\boldsymbol{\zeta},\boldsymbol{\zeta}\rangle_\Omega + \frac{C_1}{2}\langle\nabla\times\boldsymbol{\psi},\boldsymbol{\zeta}\rangle_\Omega + C_1\mu_0\,\langle\boldsymbol{\phi},\boldsymbol{\zeta}\rangle_\omega\\
&\quad= \alpha\mu_0\langle\boldsymbol{\phi},\boldsymbol{\phi}\rangle_\omega + \mu_0 C_e\theta k\,\langle\nabla\boldsymbol{\phi},\nabla\boldsymbol{\phi}\rangle_\omega + \big(C_1\mu_0 - \frac{\mu_0}{2}\big)\langle\boldsymbol{\phi},\boldsymbol{\zeta}\rangle_\omega\\
&\qquad+ \frac{C_1\varepsilon_0}{k}\langle\boldsymbol{\psi},\boldsymbol{\psi}\rangle_\Omega + \frac{C_1\sigma}{2}\langle\boldsymbol{\psi},\boldsymbol{\psi}\rangle_\omega + \frac{C_1\mu_0}{k}\langle\boldsymbol{\zeta},\boldsymbol{\zeta}\rangle_\Omega\\
&\quad\geq \underbrace{\big(\alpha - \frac{1}{2}(C_1 - 1/2)\big)}_{=:a}\,\mu_0\|\boldsymbol{\phi}\|^2_{L^2(\omega)} + \frac{C_1\varepsilon_0}{k}\|\boldsymbol{\psi}\|^2_{L^2(\Omega)}\\
&\qquad+ \underbrace{\big(\frac{C_1}{k} - \frac{C_1 - 1/2}{2}\big)}_{=:b}\,\mu_0\|\boldsymbol{\zeta}\|^2_{L^2(\omega)},
\end{aligned}$$

where we have used $\langle\boldsymbol{\phi},\boldsymbol{\zeta}\rangle_\omega \geq -\frac{1}{2}\|\boldsymbol{\phi}\|^2_{L^2(\omega)} - \frac{1}{2}\|\boldsymbol{\zeta}\|^2_{L^2(\omega)}$. Choosing $C_1 = 1/2$ now yields $a, b > 0$ and thus the desired result. ∎

ETNA
Kent State University
http://etna.math.kent.edu

The following lemma states an analogous result for the second algorithm. The proof is straightforward and we refer to the extended preprint [9] for details.

LEMMA 4.4. *Algorithm 4.2 is well defined in the sense that it admits a unique solution at each step $j = 0, \dots, N-1$ of the iterative loop.*

5. Main result and convergence analysis. In this section, we aim to show that the two preceding algorithms indeed define convergent schemes. We first consider Algorithm 4.2. The proofs within the analysis of Algorithm 4.1 are mostly omitted since they are straightforward and exactly follow the analysis of Algorithm 4.2. We again refer to the extended preprint [9] for details.

5.1. Main result. We start by collecting some general assumptions. Throughout, we assume that the spatial meshes $\mathcal{T}_h|_\omega$ are uniformly shape regular and satisfy the angle condition

$$\int_\omega \nabla\zeta_i \cdot \nabla\zeta_j \le 0 \qquad \text{for all hat functions } \zeta_i, \zeta_j \in \mathcal{S}^1(\mathcal{T}_h|_\omega) \text{ with } i \neq j. \tag{5.1}$$

For $\mathbf{x} \in \Omega$ and $t \in [t_j, t_{j+1})$, we now define for $\gamma_h^\ell \in \{\mathbf{m}_h^\ell, \mathbf{H}_h^\ell, \mathbf{E}_h^\ell, \mathbf{J}^\ell, \mathbf{v}_h^\ell\}$ the time approximations

$$\begin{aligned} &\gamma_{hk}(t,\mathbf{x}) := \frac{t-t_j}{k}\gamma_h^{j+1}(\mathbf{x}) + \frac{t_{j+1}-t}{k}\gamma_h^j(\mathbf{x}), \qquad \gamma_{hk}^-(t,\mathbf{x}) := \gamma_h^j(\mathbf{x}), \\ &\gamma_{hk}^+(t,\mathbf{x}) := \gamma_h^{j+1}(\mathbf{x}), \qquad \overline{\gamma}_{hk}(t,\mathbf{x}) := \gamma_h^{j+1/2}(\mathbf{x}) = \frac{\gamma_h^{j+1}(\mathbf{x}) + \gamma_h^j(\mathbf{x})}{2}. \end{aligned} \tag{5.2}$$

We suppose that the general energy contribution $\pi(\cdot)$ is uniformly bounded in $\mathbf{L}^2(\omega_T)$, i.e.,

$$\|\pi(\mathbf{n})\|_{\mathbf{L}^2(\omega_T)}^2 \le C_\pi \qquad \text{for all } \mathbf{n} \in \mathbf{L}^2(\omega_T) \text{ with } \|\mathbf{n}\|_{\mathbf{L}^2(\omega_T)}^2 \le 1 \tag{5.3}$$

with an (h,k)-independent constant $C_\pi > 0$ as well as

$$\pi(\mathbf{n}_{hk}) \rightharpoonup \pi(\mathbf{n}) \qquad \text{weakly subconvergent in } \mathbf{L}^2(\omega_T), \tag{5.4}$$

provided that the sequence $\mathbf{n}_{hk} \rightharpoonup \mathbf{n}$ is weakly subconvergent in $\mathbf{H}^1(\omega_T)$ towards some $\mathbf{n} \in \mathbf{H}^1(\omega_T)$. For the initial data, we assume

$$\mathbf{m}_h^0 \rightharpoonup \mathbf{m}^0 \qquad \text{weakly in } \mathbf{H}^1(\omega), \tag{5.5}$$

as well as

$$\mathbf{H}_h^0 \rightharpoonup \mathbf{H}^0 \quad \text{and} \quad \mathbf{E}_h^0 \rightharpoonup \mathbf{E}^0 \qquad \text{weakly in } \mathbf{L}^2(\Omega). \tag{5.6}$$

Finally, for the field $\mathbf{J}$, we assume sufficient regularity, e.g., $\mathbf{J} \in C\big([0,T];\mathbf{L}^2(\Omega)\big)$, such that

$$\mathbf{J}^\pm \rightharpoonup \mathbf{J} \qquad \text{weakly in } \mathbf{L}^2(\Omega_T). \tag{5.7}$$

REMARK 5.1. Before proceeding to the actual proof, we would like to remark on the before mentioned assumptions.

(i) We emphasize that all energy contributions mentioned in the introduction fulfill the assumptions (5.3)–(5.4) on $\pi(\cdot)$; cf. [16].
(ii) As in [16], the analysis can be extended to include approximations π_h of the general field contribution π. In this case, one needs to ensure uniform boundedness of those approximations as well as the subconvergence property $\pi_h(\mathbf{n}_{hk}) \rightharpoonup \pi(\mathbf{n})$ weakly in $\mathbf{L}^2(\omega_T)$ provided $\mathbf{n}_{hk}$ is weakly subconvergent to $\mathbf{n}$ in $\mathbf{H}^1(\omega_T)$.

ETNA
Kent State University
http://etna.math.kent.edu

(iii) The angle condition (5.1) is a somewhat technical but crucial ingredient for the convergence analysis. Starting from the energy decay relation

$$\int_\omega \Big|\nabla\Big(\frac{\mathbf{m}}{|\mathbf{m}|}\Big)\Big|^2 \le \int_\omega |\nabla \mathbf{m}|^2,$$

which is true for any function $\mathbf{m}$ with $|\mathbf{m}| \ge 1$ almost everywhere, it has first been shown in [11], that (5.1) and nodewise projection ensures energy decay even on a discrete level, i.e.,

$$\int_\omega \Big|\nabla \mathcal{I}_h\Big(\frac{\mathbf{m}}{|\mathbf{m}|}\Big)\Big|^2 \le \int_\omega |\nabla \mathcal{I}_h \mathbf{m}|^2.$$

This yields the inequality $\|\nabla \mathbf{m}_h^{j+1}\|^2_{\mathbf{L}^2(\omega)} \le \|\nabla \mathbf{m}_h^j + k\mathbf{v}_h^j\|^2_{\mathbf{L}^2(\omega)}$, which is needed in the upcoming proof.

(iv) Note that assumption (5.1) is automatically fulfilled for tetrahedral meshes with dihedral angles that are smaller than $\pi/2$. If the condition is satisfied by $\mathcal{T}_0$, it can be ensured for the refined meshes as well, provided, e.g., the strategy from [36, Section 4.1] is used for refinement.

(v) Inspired by [12], it has recently been proved [1] that the nodal projection step in Algorithm 4.1 and Algorithm 4.2 can be omitted. Then, the following convergence theorem remains valid even if the angle condition (5.1) is violated.

The next statement is the main theorem of this work.

THEOREM 5.2 (Convergence theorem). *Let $(\mathbf{m}_{hk}, \mathbf{v}_{hk}, \mathbf{H}_{hk}, \mathbf{E}_{hk})$ be the quantities obtained by either Algorithm 4.1 or 4.2 and assume (5.1)–(5.7) and $\theta \in (1/2, 1]$. Then, as $(h,k) \to (0,0)$ independently of each other, a subsequence of $(\mathbf{m}_{hk}, \mathbf{H}_{hk}, \mathbf{E}_{hk})$ converges weakly in $\mathbf{H}^1(\omega_T) \times \mathbf{L}^2(\Omega_T) \times \mathbf{L}^2(\Omega_T)$ to a weak solution $(\mathbf{m}, \mathbf{H}, \mathbf{E})$ of MLLG. In particular, each accumulation point of $(\mathbf{m}_{hk}, \mathbf{H}_{hk}, \mathbf{E}_{hk})$ is a weak solution of MLLG in the sense of Definition 2.1.*

The proof will roughly be done in three steps for either algorithm:

(i) Boundedness of the discrete quantities and energies.
(ii) Existence of weakly convergent subsequences.
(iii) Identification of the limits as weak solutions of MLLG.

Throughout the proof, we will apply the following discrete version of Gronwall's inequality.

LEMMA 5.3 (Gronwall). *Let $k_0, \dots, k_{r-1} > 0$ and $a_0, \dots, a_{r-1}, b, C > 0$, and let those quantities fulfill $a_0 \le b$ and $a_\ell \le b + C\sum_{j=0}^{\ell-1} k_j a_j$ for $\ell = 1, \dots, r$. Then, we have $a_\ell \le C \exp\Big(C\sum_{j=0}^{\ell-1} k_j\Big)$ for $\ell = 1, \dots, r$.*

ETNA
Kent State University
http://etna.math.kent.edu

5.2. Analysis of Algorithm 4.2. As mentioned before, we first show the desired boundedness.

LEMMA 5.4. *There exists $k_0 > 0$ such that for all $k < k_0$, the discrete quantities $(\mathbf{m}_h^j, \mathbf{E}_h^j, \mathbf{H}_h^j) \in \mathcal{M}_h \times \mathcal{X}_h \times \mathcal{Y}_h$ fulfill*

$$\begin{aligned} &\|\nabla \mathbf{m}_h^j\|_{\mathbf{L}^2(\omega)}^2 + k\sum_{i=0}^{j-1} \|\mathbf{v}_h^i\|_{\mathbf{L}^2(\omega)}^2 \\ &\quad + \|\mathbf{H}_h^j\|_{\mathbf{L}^2(\Omega)}^2 + \|\mathbf{E}_h^j\|_{\mathbf{L}^2(\Omega)}^2 + \big(\theta - 1/2\big)k^2 \sum_{i=0}^{j-1} \|\nabla \mathbf{v}_h^i\|_{\mathbf{L}^2(\omega)}^2 \\ &\quad + \sum_{i=0}^{j-1} \big(\|\mathbf{H}_h^{i+1} - \mathbf{H}_h^i\|_{\mathbf{L}^2(\Omega)}^2 + \|\mathbf{E}_h^{i+1} - \mathbf{E}_h^i\|_{\mathbf{L}^2(\Omega)}^2\big) \le C_2 \end{aligned} \tag{5.8}$$

for each $j = 0, \dots, N$ and some constant $C_2 > 0$ that only depends on $|\Omega|$, on $|\omega|$, as well as on C_π.

Proof. For the Maxwell equations, i.e., step (iii) of Algorithm 4.2, we choose the special pair of test functions $(\boldsymbol{\psi}_h, \boldsymbol{\zeta}_h) = (\mathbf{E}_h^{i+1}, \mathbf{H}_h^{i+1})$ and get from (4.2b)–(4.2c)

$$\frac{\varepsilon_0}{k}\langle \mathbf{E}_h^{i+1} - \mathbf{E}_h^i, \mathbf{E}_h^{i+1}\rangle_\Omega - \langle \mathbf{H}_h^{i+1}, \nabla \times \mathbf{E}_h^{i+1}\rangle_\Omega + \sigma\langle \chi_\omega \mathbf{E}_h^{i+1}, \mathbf{E}_h^{i+1}\rangle_\Omega = -\langle \mathbf{J}^i, \mathbf{E}_h^{i+1}\rangle_\Omega$$

and

$$\frac{\mu_0}{k}\langle \mathbf{H}_h^{i+1} - \mathbf{H}_h^i, \mathbf{H}_h^{i+1}\rangle_\Omega + \langle \nabla \times \mathbf{E}_h^{i+1}, \mathbf{H}_h^{i+1}\rangle_\Omega = -\mu_0\langle \mathbf{v}_h^i, \mathbf{H}_h^{i+1}\rangle_\omega.$$

Summing up those two equations (and multiplying by $1/C_e$), we therefore see

$$\begin{aligned} &\frac{\varepsilon_0}{kC_e}\langle \mathbf{E}_h^{i+1} - \mathbf{E}_h^i, \mathbf{E}_h^{i+1}\rangle_\Omega + \frac{\sigma}{C_e}\|\mathbf{E}_h^{i+1}\|_{\mathbf{L}^2(\omega)}^2 + \frac{\mu_0}{kC_e}\langle \mathbf{H}_h^{i+1} - \mathbf{H}_h^i, \mathbf{H}_h^{i+1}\rangle_\Omega \\ &\qquad = -\frac{\mu_0}{C_e}\langle \mathbf{v}_h^i, \mathbf{H}_h^i\rangle_\omega + \frac{\mu_0}{C_e}\langle \mathbf{v}_h^i, \mathbf{H}_h^i - \mathbf{H}_h^{i+1}\rangle_\omega - \frac{1}{C_e}\langle \mathbf{J}^i, \mathbf{E}_h^{i+1}\rangle_\Omega. \end{aligned} \tag{5.9}$$

The LLG equation (4.2a) is now tested with $\boldsymbol{\varphi}_i = \mathbf{v}_h^i \in \mathcal{K}_{\mathbf{m}_h^i}$. We get

$$\begin{aligned} &\alpha\langle \mathbf{v}_h^i, \mathbf{v}_h^i\rangle_\omega + \underbrace{\langle \mathbf{m}_h^i \times \mathbf{v}_h^i, \mathbf{v}_h^i\rangle_\omega}_{=0} \\ &\qquad = -C_e\langle \nabla(\mathbf{m}_h^i + \theta k \mathbf{v}_h^i), \nabla \mathbf{v}_h^i\rangle_\omega + \langle \mathbf{H}_h^i, \mathbf{v}_h^i\rangle_\omega + \langle \pi(\mathbf{m}_h^i), \mathbf{v}_h^i\rangle_\omega, \end{aligned}$$

whence

$$\begin{aligned} &\frac{\alpha k}{C_e}\|\mathbf{v}_h^i\|_{\mathbf{L}^2(\omega)}^2 + \theta k^2 \|\nabla \mathbf{v}_h^i\|_{\mathbf{L}^2(\omega)}^2 \\ &\qquad = -k\langle \nabla \mathbf{m}_h^i, \nabla \mathbf{v}_h^i\rangle_\omega + \frac{k}{C_e}\langle \mathbf{H}_h^i, \mathbf{v}_h^i\rangle_\omega + \frac{k}{C_e}\langle \pi(\mathbf{m}_h^i), \mathbf{v}_h^i\rangle_\omega. \end{aligned}$$

Next, along the lines of [2, 3, 16], we use the fact that $\|\nabla \mathbf{m}_h^{i+1}\|_{\mathbf{L}^2(\omega)}^2 \le \|\nabla(\mathbf{m}_h^i + k\mathbf{v}_h^i)\|_{\mathbf{L}^2(\omega)}^2$ stemming from the mesh condition (5.1), cf. [11], to see

$$\begin{aligned} \frac{1}{2}\|\nabla \mathbf{m}_h^{i+1}\|_{\mathbf{L}^2(\omega)}^2 &\le \frac{1}{2}\|\nabla \mathbf{m}_h^i\|_{\mathbf{L}^2(\omega)}^2 + k\,\langle \nabla \mathbf{m}_h^i, \nabla \mathbf{v}_h^i\rangle_\omega + \frac{k^2}{2}\|\nabla \mathbf{v}_h^i\|_{\mathbf{L}^2(\omega)} \\ &= \frac{1}{2}\|\nabla \mathbf{m}_h^i\|_{\mathbf{L}^2(\omega)}^2 - \big(\theta - 1/2\big)k^2\|\nabla \mathbf{v}_h^i\|_{\mathbf{L}^2(\omega)}^2 \\ &\quad - \frac{\alpha\, k}{C_e}\|\mathbf{v}_h^i\|_{\mathbf{L}^2(\omega)}^2 + \frac{k}{C_e}\langle \mathbf{H}_h^i, \mathbf{v}_h^i\rangle_\omega + \frac{k}{C_e}\langle \pi(\mathbf{m}_h^i), \mathbf{v}_h^i\rangle_\omega. \end{aligned}$$

ETNA
Kent State University
http://etna.math.kent.edu

Multiplying the last estimate by μ_0/k and adding (5.9), we obtain

$$
\begin{aligned}
&\frac{\mu_0}{2k}(\|\nabla \mathbf{m}_h^{i+1}\|_{\mathbf{L}^2(\omega)}^2 - \|\nabla \mathbf{m}_h^{i}\|_{\mathbf{L}^2(\omega)}^2) \\
&\quad + \big(\theta - 1/2\big)\mu_0 k \|\nabla \mathbf{v}_h^i\|_{\mathbf{L}^2(\omega)}^2 + \frac{\alpha\mu_0}{C_e}\|\mathbf{v}_h^i\|_{\mathbf{L}^2(\omega)}^2 \\
&\quad + \frac{\varepsilon_0}{k\,C_e}\langle \mathbf{E}_h^{i+1} - \mathbf{E}_h^i, \mathbf{E}_h^{i+1}\rangle_\Omega + \frac{\sigma}{C_e}\|\mathbf{E}_h^{i+1}\|_{\mathbf{L}^2(\omega)}^2 + \frac{\mu_0}{kC_e}\langle \mathbf{H}_h^{i+1} - \mathbf{H}_h^i, \mathbf{H}_h^{i+1}\rangle_\Omega \\
&\le \frac{\mu_0}{C_e}\langle \mathbf{H}_h^i - \mathbf{H}_h^{i+1}, \mathbf{v}_h^i\rangle_\omega - \frac{1}{C_e}\langle \mathbf{J}^i, \mathbf{E}_h^{i+1}\rangle_\Omega + \frac{\mu_0}{C_e}\langle \pi(\mathbf{m}_h^i), \mathbf{v}_h^i\rangle_\omega.
\end{aligned}
\tag{5.10}
$$

Next, we recall Abel's summation by parts, i.e., for arbitrary $\boldsymbol{u}_i \in \mathbb{R}^n$ and $j \ge 0$, there holds

$$
\sum_{i=1}^{j}(\boldsymbol{u}_i - \boldsymbol{u}_{i-1})\cdot \boldsymbol{u}_i = \frac{1}{2}|\boldsymbol{u}_j|^2 - \frac{1}{2}|\boldsymbol{u}_0|^2 + \frac{1}{2}\sum_{i=1}^{j}|\boldsymbol{u}_i - \boldsymbol{u}_{i-1}|^2.
$$

Multiplying the above equation (5.10) by k, summing up over the time intervals, and exploiting Abel's summation for the $\mathbf{E}_h^i$ and $\mathbf{H}_h^i$ scalar-products yields

$$
\begin{aligned}
&\frac{\mu_0}{2}\|\nabla \mathbf{m}_h^j\|_{\mathbf{L}^2(\omega)}^2 + \big(\theta - 1/2\big)\mu_0 k^2 \sum_{i=0}^{j-1}\|\nabla \mathbf{v}_h^i\|_{\mathbf{L}^2(\omega)}^2 \\
&\quad + \frac{\alpha k\mu_0}{C_e}\sum_{i=0}^{j-1}\|\mathbf{v}_h^i\|_{\mathbf{L}^2(\omega)}^2 + \frac{\varepsilon_0}{2C_e}\|\mathbf{E}_h^j\|_{\mathbf{L}^2(\Omega)}^2 \\
&\quad + \frac{\varepsilon_0}{2C_e}\sum_{i=0}^{j-1}\|\mathbf{E}_h^{i+1} - \mathbf{E}_h^i\|_{\mathbf{L}^2(\Omega)}^2 + \frac{k\sigma}{C_e}\sum_{i=0}^{j-1}\|\mathbf{E}_h^{i+1}\|_{\mathbf{L}^2(\omega)}^2 \\
&\quad + \frac{\mu_0}{2C_e}\|\mathbf{H}_h^j\|_{\mathbf{L}^2(\Omega)}^2 + \frac{\mu_0}{2C_e}\sum_{i=0}^{j-1}\|\mathbf{H}_h^{i+1} - \mathbf{H}_h^i\|_{\mathbf{L}^2(\Omega)}^2 \\
&\le \frac{\mu_0 k}{C_e}\sum_{i=0}^{j-1}\langle \mathbf{H}_h^i - \mathbf{H}_h^{i+1}, \mathbf{v}_h^i\rangle_\omega - \frac{k}{C_e}\sum_{i=0}^{j-1}\langle \mathbf{J}^i, \mathbf{E}_h^{i+1}\rangle_\Omega + \frac{\mu_0 k}{C_e}\sum_{i=0}^{j-1}\langle \pi(\mathbf{m}_h^i), \mathbf{v}_h^i\rangle_\omega \\
&\quad + \underbrace{\frac{\mu_0}{2}\|\nabla \mathbf{m}_h^0\|_{\mathbf{L}^2(\omega)}^2 + \frac{\varepsilon_0}{2C_e}\|\mathbf{E}_h^0\|_{\mathbf{L}^2(\Omega)}^2 + \frac{\mu_0}{2C_e}\|\mathbf{H}_h^0\|_{\mathbf{L}^2(\Omega)}^2}_{=:\mathcal{E}_h^0}
\end{aligned}
$$

for any $j \in 1, \dots, N$. By use of the inequalities of Young and Hölder, the first part of the right-hand side can be estimated by

$$
\begin{aligned}
&\frac{k\mu_0}{C_e}\sum_{i=0}^{j-1}\langle \mathbf{H}_h^i - \mathbf{H}_h^{i+1}, \mathbf{v}_h^i\rangle_\omega - \frac{k}{C_e}\sum_{i=0}^{j-1}\langle \mathbf{J}^i, \mathbf{E}_h^{i+1}\rangle_\Omega + \frac{\mu_0 k}{C_e}\sum_{i=0}^{j-1}\langle \pi(\mathbf{m}_h^i), \mathbf{v}_h^i\rangle_\omega \\
&\quad \le \frac{k\mu_0}{C_e}\sum_{i=0}^{j-1}\frac{1}{2\delta_1}(\|\pi(\mathbf{m}_h^i)\|_{\mathbf{L}^2(\omega)}^2 + \|\mathbf{H}_h^{i+1} - \mathbf{H}_h^i\|_{\mathbf{L}^2(\Omega)}^2) + \frac{\delta_1\mu_0 k}{C_e}\sum_{i=0}^{j-1}\|\mathbf{v}_h^i\|_{\mathbf{L}^2(\omega)}^2 \\
&\qquad + \frac{k}{4\delta_2 C_e}\sum_{i=0}^{j-1}\|\mathbf{E}_h^{i+1}\|_{\mathbf{L}^2(\Omega)}^2 + \frac{\delta_2 k}{C_e}\sum_{i=0}^{j-1}\|\mathbf{J}^i\|_{\mathbf{L}^2(\Omega)}^2,
\end{aligned}
$$

for any $\delta_1, \delta_2 > 0$. The combination of the last two estimates yields

ETNA
Kent State University
http://etna.math.kent.edu

$$
\begin{aligned}
&\frac{\mu_0}{2}\|\nabla \mathbf{m}_h^j\|_{\mathbf{L}^2(\omega)}^2 + \big(\theta - 1/2\big)\mu_0 k^2 \sum_{i=0}^{j-1} \|\nabla \mathbf{v}_h^i\|_{\mathbf{L}^2(\omega)}^2 \\
&\qquad + \frac{\alpha k \mu_0}{C_e} \sum_{i=0}^{j-1} \|\mathbf{v}_h^i\|_{\mathbf{L}^2(\omega)}^2 + \frac{\varepsilon_0}{2C_e}\|\mathbf{E}_h^j\|_{\mathbf{L}^2(\Omega)}^2 \\
&\qquad + \frac{\varepsilon_0}{2C_e} \sum_{i=0}^{j-1} \|\mathbf{E}_h^{i+1} - \mathbf{E}_h^i\|_{\mathbf{L}^2(\Omega)}^2 + \frac{k\sigma}{C_e} \sum_{i=0}^{j-1} \|\mathbf{E}_h^{i+1}\|_{\mathbf{L}^2(\omega)}^2 + \frac{\mu_0}{2C_e}\|\mathbf{H}_h^j\|_{\mathbf{L}^2(\Omega)}^2 \\
&\qquad + \frac{\mu_0}{2C_e} \sum_{i=0}^{j-1} \|\mathbf{H}_h^{i+1} - \mathbf{H}_h^i\|_{\mathbf{L}^2(\Omega)}^2 \\
&\le \frac{\mu_0}{2C_e\delta_1} k \sum_{i=0}^{j-1} (\|\pi(\mathbf{m}_h^i)\|_{\mathbf{L}^2(\omega)}^2 + \|\mathbf{H}_h^{i+1} - \mathbf{H}_h^i\|_{\mathbf{L}^2(\Omega)}^2) + \frac{\delta_1 \mu_0 k}{C_e} \sum_{i=0}^{j-1} \|\mathbf{v}_h^i\|_{\mathbf{L}^2(\omega)}^2 \\
&\qquad + \frac{k\delta_2}{C_e} \sum_{i=0}^{j-1} \|\mathbf{E}_h^{i+1}\|_{\mathbf{L}^2(\Omega)}^2 + \frac{k}{4\delta_2 C_e} \sum_{i=0}^{j-1} \|\mathbf{J}^i\|_{\mathbf{L}^2(\Omega)}^2 + \mathcal{E}_h^0.
\end{aligned}
$$

Unfortunately, the term $\frac{k\delta_2}{C_e}\sum_{i=0}^{j-1}\|\mathbf{E}_h^{i+1}\|_{\mathbf{L}^2(\Omega)}^2$ on the right-hand side cannot be absorbed by the term $\frac{k\sigma}{C_e}\sum_{i=0}^{j-1}\|\mathbf{E}_h^{i+1}\|_{\mathbf{L}^2(\omega)}^2$ on the left-hand side since the latter consists only of contributions on the smaller domain ω. The remedy is to artificially enlarge the first term by

$$
\frac{k\delta_2}{C_e} \sum_{i=0}^{j-1} \|\mathbf{E}_h^{i+1}\|_{\mathbf{L}^2(\Omega)}^2 \le \frac{2k\delta_2}{C_e} \sum_{i=0}^{j-1} \|\mathbf{E}_h^{i+1} - \mathbf{E}_h^i\|_{\mathbf{L}^2(\Omega)}^2 + \frac{2\delta_2 k}{C_e} \sum_{i=0}^{j-1} \|\mathbf{E}_h^i\|_{\mathbf{L}^2(\Omega)}^2
$$

and absorb the first sum into the corresponding quantity on the left-hand side. With

$$
C_{\mathbf{v}} := \frac{\mu_0 k}{C_e}(\alpha - \delta_1), \quad C_{\mathbf{H}} := \frac{\mu_0}{2C_e}\big(1 - \frac{k}{\delta_1}\big), \quad \text{and} \quad C_{\mathbf{E}} := \frac{1}{2C_e}\big(\varepsilon_0 - 4\delta_2 k\big),
$$

this yields

$$
\begin{aligned}
a_j &:= \frac{\mu_0}{2}\|\nabla \mathbf{m}_h^j\|_{\mathbf{L}^2(\omega)}^2 + \big(\theta - 1/2\big)\mu_0 k^2 \sum_{i=0}^{j-1} \|\nabla \mathbf{v}_h^i\|_{\mathbf{L}^2(\omega)}^2 + C_{\mathbf{v}} \sum_{i=0}^{j-1} \|\mathbf{v}_h^i\|_{\mathbf{L}^2(\omega)}^2 \\
&\qquad + \frac{\varepsilon_0}{2C_e}\|\mathbf{E}_h^j\|_{\mathbf{L}^2(\Omega)}^2 + C_{\mathbf{E}} \sum_{i=0}^{j-1} \|\mathbf{E}_h^{i+1} - \mathbf{E}_h^i\|_{\mathbf{L}^2(\Omega)}^2 + \frac{k\sigma}{C_e} \sum_{i=0}^{j-1} \|\mathbf{E}_h^{i+1}\|_{\mathbf{L}^2(\omega)}^2 \\
&\qquad + \frac{\mu_0}{2C_e}\|\mathbf{H}_h^j\|_{\mathbf{L}^2(\Omega)}^2 + C_{\mathbf{H}} \sum_{i=0}^{j-1} \|\mathbf{H}_h^{i+1} - \mathbf{H}_h^i\|_{\mathbf{L}^2(\Omega)}^2 \\
&\le \underbrace{\mathcal{E}_h^0 + \frac{k\mu_0}{2C_e\delta_1} \sum_{i=0}^{j-1} \|\pi(\mathbf{m}_h^i)\|_{\mathbf{L}^2(\omega)}^2 + \frac{k}{4\delta_2 C_e} \sum_{i=0}^{j-1} \|\mathbf{J}^i\|_{\mathbf{L}^2(\Omega)}^2}_{=:b} + \frac{2\delta_2 k}{C_e} \sum_{i=0}^{j-1} \|\mathbf{E}_h^i\|_{\mathbf{L}^2(\Omega)}^2 \\
&\le b + \frac{4\delta_2 k}{\varepsilon_0} \sum_{i=0}^{j-1} a_i.
\end{aligned}
$$

ETNA
Kent State University
http://etna.math.kent.edu

In order to show the desired result, we have to ensure that there are choices of δ_1 and δ_2, such that the constants $C_{\mathbf{v}}, C_{\mathbf{H}}$, and $C_{\mathbf{E}}$ are positive, i.e.,

$$(\alpha - \delta_1) > 0, \quad \big(1 - \frac{k}{\delta_1}\big) > 0, \quad \text{and} \quad (\varepsilon_0 - 4\delta_2 k) > 0,$$

which is equivalent to $k_0 < \delta_1 < \alpha$ and $\delta_2 < \varepsilon_0/4k_0$. The application of the discrete Gronwall inequality from Lemma 5.3 yields $a_j \le M$ and thus proves the desired result. ∎

We can now conclude the existence of weakly convergent subsequences.

LEMMA 5.5. *There exist functions* $(\mathbf{m}, \mathbf{H}, \mathbf{E}) \in \mathbf{H}^1(\omega_T, \mathbb{S}^2) \times \mathbf{L}^2(\Omega_T) \times \mathbf{L}^2(\Omega_T)$ *such that*

$$\begin{aligned}
\mathbf{m}_{hk} &\rightharpoonup \mathbf{m} && \text{in } \mathbf{H}^1(\omega_T),\\
\mathbf{m}_{hk}, \mathbf{m}_{hk}^{\pm}, \overline{\mathbf{m}}_{hk} &\rightharpoonup \mathbf{m} && \text{in } L^2(\mathbf{H}^1(\omega)),\\
\mathbf{m}_{hk}, \mathbf{m}_{hk}^{\pm}, \overline{\mathbf{m}}_{hk} &\to \mathbf{m} && \text{in } \mathbf{L}^2(\omega_T),\\
\mathbf{H}_{hk}, \mathbf{H}_{hk}^{\pm}, \overline{\mathbf{H}}_{hk} &\rightharpoonup \mathbf{H} && \text{in } \mathbf{L}^2(\Omega_T),\\
\mathbf{E}_{hk}, \mathbf{E}_{hk}^{\pm}, \overline{\mathbf{E}}_{hk} &\rightharpoonup \mathbf{H} && \text{in } \mathbf{L}^2(\Omega_T),
\end{aligned}$$

where the subsequences are successively constructed, i.e., for arbitrary mesh sizes $h \to 0$ *and time step sizes* $k \to 0$ *there exist subindices* h_ℓ, k_ℓ *for which the above convergence properties are satisfied simultaneously. In addition, there exist some* $\mathbf{v} \in \mathbf{L}^2(\omega_\tau)$ *with*

$$\mathbf{v}_{hk}^{-} \rightharpoonup \mathbf{v} \text{ in } \mathbf{L}^2(\omega_T)$$

for the same subsequence as above.

Proof. From Lemma 5.4, we immediately get uniform boundedness of all of those sequences. A compactness argument thus allows us to successively extract weakly convergent subsequences. It only remains to show that the corresponding limits coincide, i.e.,

$$\lim \gamma_{hk} = \lim \gamma_{hk}^{-} = \lim \gamma_{hk}^{+} = \lim \overline{\gamma}_{hk}, \qquad \text{where } \gamma_{hk} \in \{\mathbf{m}_{hk}, \mathbf{H}_{hk}, \mathbf{E}_{hk}\}.$$

In particular, Lemma 5.4 provides the uniform bound

$$\sum_{i=0}^{j-1} \|\mathbf{m}_h^{i+1} - \mathbf{m}_h^i\|_{\mathbf{L}^2(\omega)}^2 \le C_2.$$

Here, we used the fact that $\|\mathbf{m}_h^{j+1} - \mathbf{m}_h^j\|_{\mathbf{L}^2(\omega)}^2 \le k^2 \|\mathbf{v}_h^j\|_{\mathbf{L}^2(\omega)}^2$; see, e.g., [2] or [24, Lemma 3.3.2]. We rewrite $\gamma_{hk} \in \{\mathbf{m}_{hk}, \mathbf{E}_{hk}, \mathbf{H}_{hk}\}$ as $\gamma_h^j + \frac{t-t_j}{k}(\gamma_h^{j+1} - \gamma_h^j)$ on $[t_{j-1}, t_j]$ and thus get

$$\begin{aligned}
\|\gamma_{hk} - \gamma_{hk}^{-}\|_{\mathbf{L}^2(\Omega_T)}^2 &= \sum_{j=0}^{N-1} \int_{t_j}^{t_{j+1}} \|\gamma_h^j + \frac{t-t_j}{k}(\gamma_h^{j+1} - \gamma_h^j) - \gamma_h^j\|_{\mathbf{L}^2(\Omega)}^2\\
&\le k \sum_{j=0}^{N-1} \|\gamma_h^{j+1} - \gamma_h^j\|_{\mathbf{L}^2(\Omega)}^2 \longrightarrow 0
\end{aligned}$$

and analogously

$$\|\gamma_{hk} - \gamma_{hk}^{+}\|_{\mathbf{L}^2(\Omega_T)}^2 \longrightarrow 0,$$

ETNA
Kent State University
http://etna.math.kent.edu

i.e., we have $\lim \gamma_{hk}^{\pm} = \lim \gamma_{hk} \in \mathbf{L}^2(\Omega_T)$ respectively $\mathbf{L}^2(\omega_T)$. In particular, it holds that $\lim \overline{\gamma}_{hk} = \lim \gamma_{hk}$. From the uniqueness of weak limits and the continuous inclusions $\mathbf{H}^1(\omega_T) \subseteq L^2(\mathbf{H}^1(\omega)) \subseteq \mathbf{L}^2(\omega_T)$, we then even conclude the convergence properties of $\mathbf{m}_{hk}$, $\mathbf{m}_{hk}^{\pm}$, and $\overline{\mathbf{m}}_{hk}$ in $\mathbf{L}^2(\mathbf{H}^1(\omega))$ as well as $\mathbf{m}_{hk} \rightharpoonup \mathbf{m}$ in $\mathbf{H}^1(\omega_T)$. From

$$\| |\mathbf{m}| - 1 \|_{\mathbf{L}^2(\omega_T)} \le \| |\mathbf{m}| - |\mathbf{m}_{hk}^-| \|_{\mathbf{L}^2(\omega_T)} + \| |\mathbf{m}_{hk}^-| - 1 \|_{\mathbf{L}^2(\omega_T)}$$

and

$$\| |\mathbf{m}_{hk}^-(t,\cdot)| - 1 \|_{\mathbf{L}^2(\omega)} \le h \max_{t_j} \|\nabla \mathbf{m}_h^j\|_{\mathbf{L}^2(\omega)},$$

we finally deduce $|\mathbf{m}| = 1$ almost everywhere in ω_T. ∎

LEMMA 5.6. *The limit function* $\mathbf{v} \in \mathbf{L}^2(\omega_T)$ *equals the time derivative of* $\mathbf{m}$*, i.e.,* $\mathbf{v} = \partial_t \mathbf{m}$ *almost everywhere in* ω_T.

Proof. The proof follows the lines of [2] and we therefore only sketch it. The elaborated arguments can be found in [24, Lemma 3.3.12]. Using the inequality

$$\|\partial_t \mathbf{m}_{hk} - \mathbf{v}_{hk}^-\|_{\mathbf{L}^1(\omega_T)} \lesssim \frac{1}{2} k \|\mathbf{v}_{hk}^-\|_{\mathbf{L}^2(\omega_T)}^2,$$

we exploit weak semicontinuity of the norm to see

$$\|\partial_t \mathbf{m} - \mathbf{v}\|_{\mathbf{L}^1(\omega_T)} \le \liminf \|\partial_t \mathbf{m}_{hk} - \mathbf{v}_{hk}^-\|_{\mathbf{L}^1(\omega_T)} = 0 \qquad \text{as } (h,k) \longrightarrow (0,0),$$

whence $\mathbf{v} = \partial_t \mathbf{m}$ almost everywhere in ω_T. ∎

Proof of Theorem 5.2. For the LLG part of (2.2), we follow the lines of [2]. Let $\boldsymbol{\varphi} \in C^\infty(\omega_T)$ and $(\boldsymbol{\psi}, \boldsymbol{\zeta}) \in C_c^\infty\big([0,T); C^\infty(\overline{\Omega}) \cap \mathbf{H}_0(\mathbf{curl}, \Omega)\big)$ be arbitrary. We now define test functions by $(\boldsymbol{\phi}_h, \boldsymbol{\psi}_h, \boldsymbol{\zeta}_h)(t,\cdot) := \big(\mathcal{I}_h(\mathbf{m}_{hk}^- \times \boldsymbol{\varphi}), \mathcal{I}_{\mathcal{X}_h}\boldsymbol{\psi}, \mathcal{I}_{\mathcal{Y}_h}\boldsymbol{\zeta}\big)(t,\cdot)$. Recall that the $\mathbf{L}^2$-orthogonal projection $\mathcal{I}_{\mathcal{Y}_h} : \mathbf{L}^2(\Omega) \to \mathcal{Y}_h$ satisfies $(\mathbf{u} - \mathcal{I}_{\mathcal{Y}_h}\mathbf{u}, \mathbf{y}_h) = 0$ for all $\mathbf{y}_h \in \mathcal{Y}_h$ and all $\mathbf{u} \in \mathbf{L}^2(\Omega)$. With the notation (5.2), equation (4.2a) of Algorithm 4.2 implies

$$\begin{aligned}\alpha \int_0^T \langle \mathbf{v}_{hk}^-, \boldsymbol{\phi}_h \rangle_\omega + \int_0^T \langle \mathbf{m}_{hk}^- \times \mathbf{v}_{hk}^-, \boldsymbol{\phi}_h \rangle_\omega &= -C_e \int_0^T \langle \nabla(\mathbf{m}_{hk}^- + \theta k \mathbf{v}_{hk}^-), \nabla \boldsymbol{\phi}_h \rangle_\omega \\ &\quad + \int_0^T \langle \mathbf{H}_{hk}^-, \boldsymbol{\phi}_h \rangle_\omega + \int_0^T \langle \pi(\mathbf{m}_{hk}^-), \boldsymbol{\phi}_h \rangle_\omega.\end{aligned}$$

With $\boldsymbol{\phi}_h(t,\cdot) := \mathcal{I}_h(\mathbf{m}_{hk}^- \times \boldsymbol{\varphi})(t,\cdot)$ and the approximation properties of the nodal interpolation operator, this yields

$$\begin{aligned}&\int_0^T \langle \alpha \mathbf{v}_{hk}^- + \mathbf{m}_{hk}^- \times \mathbf{v}_{hk}^-, \mathbf{m}_{hk}^- \times \boldsymbol{\varphi} \rangle_\omega \\ &\qquad + k\,\theta \int_0^T \langle \nabla \mathbf{v}_{hk}^-, \nabla(\mathbf{m}_{hk}^- \times \boldsymbol{\varphi}) \rangle_\omega + C_e \int_0^T \langle \nabla \mathbf{m}_{hk}^-, \nabla(\mathbf{m}_{hk}^- \times \boldsymbol{\varphi}) \rangle_\omega \\ &\qquad - \int_0^T \langle \mathbf{H}_{hk}^-, \mathbf{m}_{hk}^- \times \boldsymbol{\varphi} \rangle_\omega - \int_0^T \langle \pi(\mathbf{m}_{hk}^-), \mathbf{m}_{hk}^- \times \boldsymbol{\varphi} \rangle_\omega = \mathcal{O}(h).\end{aligned}$$

Passing to the limit and using the strong $\mathbf{L}^2(\omega_T)$-convergence of $\mathbf{m}_{hk}^- \times \boldsymbol{\varphi}$ towards $\mathbf{m} \times \boldsymbol{\varphi}$,

ETNA
Kent State University
http://etna.math.kent.edu

we get

$$\int_0^T \langle \alpha \mathbf{v}_{hk}^- + \mathbf{m}_{hk}^- \times \mathbf{v}_{hk}^-, \mathbf{m}_{hk}^- \times \boldsymbol{\varphi} \rangle_\omega \longrightarrow \int_0^T \langle \alpha \mathbf{m}_t + \mathbf{m} \times \mathbf{m}_t, \mathbf{m} \times \boldsymbol{\varphi} \rangle_\omega,$$
$$k\,\theta \int_0^T \langle \nabla \mathbf{v}_{hk}^-, \nabla(\mathbf{m}_{hk}^- \times \boldsymbol{\varphi}) \rangle_\omega \longrightarrow 0, \qquad \text{and}$$
$$\int_0^T \langle \nabla \mathbf{m}_{hk}^-, \nabla(\mathbf{m}_{hk}^- \times \boldsymbol{\varphi}) \rangle_\omega \longrightarrow \int_0^T \langle \nabla \mathbf{m}, \nabla(\mathbf{m} \times \boldsymbol{\varphi}) \rangle_\omega;$$

cf. [2]. For the second limit, we have used the boundedness of $k\|\nabla \mathbf{v}_{hk}^-\|^2_{\mathbf{L}^2(\omega_T)}$ for $\theta \in (1/2, 1]$; see Lemma 5.4. The weak convergence properties of $\mathbf{H}_{hk}^-$ and $\pi(\mathbf{m}_{hk}^-)$ from (5.4) now yield

$$\int_0^T \langle \mathbf{H}_{hk}^-, \mathbf{m}_{hk}^- \times \boldsymbol{\varphi} \rangle_\omega \longrightarrow \int_0^T \langle \mathbf{H}, \mathbf{m} \times \boldsymbol{\varphi} \rangle_\omega \qquad \text{and}$$
$$\int_0^T \langle \pi(\mathbf{m}_{hk}^-), \mathbf{m}_{hk}^- \times \boldsymbol{\varphi} \rangle_\omega \longrightarrow \int_0^T \langle \pi(\mathbf{m}), \mathbf{m} \times \boldsymbol{\varphi} \rangle_\omega.$$

So far, we thus have proved

$$\int_0^T \langle \alpha \mathbf{m}_t + \mathbf{m} \times \mathbf{m}_t, \mathbf{m} \times \boldsymbol{\varphi} \rangle_\omega = -C_e \int_0^T \langle \nabla \mathbf{m}, \nabla(\mathbf{m} \times \boldsymbol{\varphi}) \rangle_\omega + \int_0^T \langle \mathbf{H}, \mathbf{m} \times \boldsymbol{\varphi} \rangle_\omega + \int_0^T \langle \pi(\mathbf{m}), \mathbf{m} \times \boldsymbol{\varphi} \rangle_\omega.$$

Finally, we use the identities

$$(\mathbf{m} \times \mathbf{m}_t) \cdot (\mathbf{m} \times \boldsymbol{\varphi}) = \mathbf{m}_t \cdot \boldsymbol{\varphi},$$
$$\mathbf{m}_t \cdot (\mathbf{m} \times \boldsymbol{\varphi}) = -(\mathbf{m} \times \mathbf{m}_t) \cdot \boldsymbol{\varphi}, \qquad \text{and}$$
$$\nabla \mathbf{m} \times \nabla(\mathbf{m} \times \boldsymbol{\varphi}) = \nabla \mathbf{m} \cdot (\mathbf{m} \times \nabla \boldsymbol{\varphi})$$

for the left-hand side respectively the first term on the right-hand side to conclude (2.2). The equality $\mathbf{m}(0, \cdot) = \mathbf{m}^0$ in the trace sense follows from the weak convergence $\mathbf{m}_{hk} \rightharpoonup \mathbf{m}$ in $\mathbf{H}^1(\omega_T)$ and thus weak convergence of the traces. Using the weak convergence $\mathbf{m}_h^0 \rightharpoonup \mathbf{m}^0$ in $\mathbf{L}^2(\omega)$, we finally identify the sought limit.

For the Maxwell part (2.3)–(2.4) of Definition 2.1, we proceed as in [7]. Given the above definition of the test functions, (4.2b) implies

$$\varepsilon_0 \int_0^T \langle (\mathbf{E}_{hk})_t, \boldsymbol{\psi}_h \rangle_\Omega - \int_0^T \langle \mathbf{H}_{hk}^+, \nabla \times \boldsymbol{\psi}_h \rangle_\Omega + \sigma \int_0^T \langle \chi_\omega \mathbf{E}_{hk}^+, \boldsymbol{\psi}_h \rangle_\Omega = \int_0^T \langle \mathbf{J}_{hk}^-, \boldsymbol{\psi}_h \rangle_\Omega,$$
$$\mu_0 \int_0^T \langle (\mathbf{H}_{hk})_t, \boldsymbol{\zeta}_h \rangle_\Omega + \int_0^T \langle \nabla \times \mathbf{E}_{hk}^+, \boldsymbol{\zeta}_h \rangle_\Omega = -\mu_0 \int_0^T \langle \mathbf{v}_{hk}^-, \boldsymbol{\zeta}_h \rangle_\omega.$$

We now consider each of those two terms separately. For the first term of the first equation, we integrate by parts in time and get

$$\int_0^T \langle (\mathbf{E}_{hk})_t, \boldsymbol{\psi}_h \rangle_\Omega = -\int_0^T \langle \mathbf{E}_{hk}, (\boldsymbol{\psi}_h)_t \rangle_\Omega + \underbrace{\langle \mathbf{E}_{hk}(T, \cdot), \boldsymbol{\psi}_h(T, \cdot) \rangle_\Omega}_{=0} - \langle \mathbf{E}_h^0, \boldsymbol{\psi}_h(0, \cdot) \rangle_\Omega.$$

ETNA
Kent State University
http://etna.math.kent.edu

Passing to the limit on the right-hand side, we see that

$$\int_0^T \langle (\mathbf{E}_{hk})_t, \boldsymbol{\psi}_h\rangle_\Omega \longrightarrow -\int_0^T \langle \mathbf{E}, \boldsymbol{\psi}_t\rangle_\Omega - \langle \mathbf{E}^0, \boldsymbol{\psi}(0,\cdot)\rangle_\Omega,$$

where we have used the assumed convergence of the initial data. For the first term in the second equation, we proceed analogously. The convergence of the terms

$$\begin{aligned}
\int_0^T \langle \mathbf{H}_{hk}^+, \nabla\times\boldsymbol{\psi}_h\rangle_\Omega &\longrightarrow \int_0^T \langle \mathbf{H}, \nabla\times\boldsymbol{\psi}\rangle_\Omega,\\
\int_0^T \langle \chi_\omega \mathbf{E}_{hk}^+, \boldsymbol{\psi}_h\rangle_\Omega &\longrightarrow \int_0^T \langle \chi_\omega \mathbf{E}, \boldsymbol{\psi}\rangle_\Omega,\\
\int_0^T \langle \mathbf{J}_{hk}^-, \boldsymbol{\psi}_h\rangle_\Omega &\longrightarrow \int_0^T \langle \mathbf{J}, \boldsymbol{\psi}\rangle_\Omega, \qquad \text{and}\\
\int_0^T \langle \mathbf{v}_{hk}^-, \boldsymbol{\zeta}_h\rangle_\omega &\longrightarrow \int_0^T \langle \mathbf{m}_t, \boldsymbol{\zeta}\rangle_\omega
\end{aligned}$$

is straightforward. Here, we have used the approximation properties (3.1)–(3.2) of the interpolation operators for the last two limits. It remains to analyze the second term in the second equation. Using $\nabla\times\mathbf{E}_{hk}^+(t)\in\mathcal{Y}_h$ and the orthogonality properties of $\mathcal{I}_{\mathcal{Y}_h}$, we deduce

$$\begin{aligned}
\int_0^T \langle \nabla\times\mathbf{E}_{hk}^+, \boldsymbol{\zeta}_h\rangle_\Omega &= \int_0^T \langle \nabla\times\mathbf{E}_{hk}^+, \boldsymbol{\zeta}\rangle_\Omega - \int_0^T \langle \nabla\times\mathbf{E}_{hk}^+, (1-\mathcal{I}_{\mathcal{Y}_h})\boldsymbol{\zeta}\rangle_\Omega\\
&= \int_0^T \langle \nabla\times\mathbf{E}_{hk}^+, \boldsymbol{\zeta}\rangle_\Omega = \int_0^T \langle \mathbf{E}_{hk}^+, \nabla\times\boldsymbol{\zeta}\rangle_\Omega \longrightarrow \int_0^T \langle \mathbf{E}, \nabla\times\boldsymbol{\zeta}\rangle_\Omega.
\end{aligned}$$

For the last equality, we have used the boundary condition $\boldsymbol{\zeta}\times\mathbf{n}=0$ on $\partial\Omega_T$ and integration by parts. This yields (2.3) and (2.4).

It remains to show the energy estimate (2.5). From the discrete energy estimate (5.8), we get for any $t'\in[0,T]$ with $t'\in[t_j,t_{j+1})$

$$\begin{aligned}
&\|\nabla\mathbf{m}_{hk}^+(t')\|_{\mathbf{L}^2(\omega)}^2 + \|\mathbf{v}_{hk}^-\|_{\mathbf{L}^2(\omega_{t'})}^2 + \|\mathbf{H}_{hk}^+(t')\|_{\mathbf{L}^2(\Omega)}^2 + \|\mathbf{E}_{hk}^+(t')\|_{\mathbf{L}^2(\Omega)}^2\\
&= \|\nabla\mathbf{m}_{hk}^+(t')\|_{\mathbf{L}^2(\omega)}^2 + \int_0^{t'} \|\mathbf{v}_{hk}^-(s)\|_{\mathbf{L}^2(\omega)}^2 + \|\mathbf{H}_{hk}^+(t')\|_{\mathbf{L}^2(\Omega)}^2 + \|\mathbf{E}_{hk}^+(t')\|_{\mathbf{L}^2(\Omega)}^2\\
&\le \|\nabla\mathbf{m}_{hk}^+(t')\|_{\mathbf{L}^2(\omega)}^2 + \int_0^{t_{j+1}} \|\mathbf{v}_{hk}^-(s)\|_{\mathbf{L}^2(\omega)}^2 + \|\mathbf{H}_{hk}^+(t')\|_{\mathbf{L}^2(\Omega)}^2 + \|\mathbf{E}_{hk}^+(t')\|_{\mathbf{L}^2(\Omega)}^2\\
&\le C_2.
\end{aligned}$$

Integration in time thus yields for any measurable set $\mathfrak{I}\subseteq[0,T]$

$$\begin{aligned}
&\int_{\mathfrak{I}} \|\nabla\mathbf{m}_{hk}^+(t')\|_{\mathbf{L}^2(\omega)}^2 + \int_{\mathfrak{I}} \|\mathbf{v}_{hk}^-\|_{\mathbf{L}^2(\omega_{t'})}^2\\
&\qquad + \int_{\mathfrak{I}} \|\mathbf{H}_{hk}^+(t')\|_{\mathbf{L}^2(\Omega)}^2 + \int_{\mathfrak{I}} \|\mathbf{E}_{hk}^+(t')\|_{\mathbf{L}^2(\Omega)}^2 \le \int_{\mathfrak{I}} C_2,
\end{aligned}$$

whence weak lower semi-continuity leads to

$$\int_{\mathfrak{I}} \|\nabla\mathbf{m}\|_{\mathbf{L}^2(\omega)}^2 + \int_{\mathfrak{I}} \|\mathbf{m}_t\|_{\mathbf{L}^2(\omega_{t'})}^2 + \int_{\mathfrak{I}} \|\mathbf{H}\|_{\mathbf{L}^2(\Omega)}^2 \int_{\mathfrak{I}} \|\mathbf{E}\|_{\mathbf{L}^2(\Omega)}^2 \le \int_{\mathfrak{I}} C_2.$$

The desired result now follows from standard measure theory; see, e.g., [21, IV, Thm. 4.4]. □

ETNA
Kent State University
http://etna.math.kent.edu

5.3. Analysis of Algorithm 4.1. This short section deals with Algorithm 4.1. Since the analysis follows the lines of Section 5.2, we omit the proofs and the reader is referred to the extended preprint of this work [9] for details. As before, we have boundedness of the involved discrete quantities, this time, however, in a slight variation.

LEMMA 5.7. *The discrete quantities* $(\mathbf{m}_h^j, \mathbf{E}_h^j, \mathbf{H}_h^j) \in \mathcal{M}_h \times \mathcal{X}_h \times \mathcal{Y}_h$ *fulfill*

$$\|\nabla \mathbf{m}_h^j\|_{\mathbf{L}^2(\omega)}^2 + k \sum_{i=0}^{j-1} \|\mathbf{v}_h^i\|_{\mathbf{L}^2(\omega)}^2 + \|\mathbf{H}_h^j\|_{\mathbf{L}^2(\Omega)}^2 + \|\mathbf{E}_h^j\|_{\mathbf{L}^2(\Omega)}^2 + \big(\theta - 1/2\big) k^2 \sum_{i=0}^{j-1} \|\nabla \mathbf{v}_h^i\|_{\mathbf{L}^2(\omega)}^2 \le C_3$$

for each $j = 0, \dots, N$ *and some constant* $C_3 > 0$ *that depends only on* $|\Omega|$, $|\omega|$, *and* C_π.

Note, that in contrast to Lemma 5.4 from the analysis of Algorithm 4.2, we do not have boundedness of $\sum_{i=0}^{j-1} (\|\mathbf{H}_h^{i+1} - \mathbf{H}_h^i\|_{\mathbf{L}^2(\Omega)}^2 + \|\mathbf{E}_h^{i+1} - \mathbf{E}_h^i\|_{\mathbf{L}^2(\Omega)}^2)$ in this case. This, however, is not necessary to prove that the limits of the in time piecewise constant and piecewise affine approximations coincide. The remedy is a clever use of the midpoint rule; details are found in [33, Section 4.2.1]. Analogously to Lemma 5.5, we thus conclude the existence of weakly convergent subsequences that fulfill

$$\begin{aligned}
\mathbf{m}_{hk} &\rightharpoonup \mathbf{m} && \text{in } \mathbf{H}^1(\omega_T),\\
\mathbf{m}_{hk}, \mathbf{m}_{hk}^{\pm}, \overline{\mathbf{m}}_{hk} &\rightharpoonup \mathbf{m} && \text{in } L^2(\mathbf{H}^1(\omega)),\\
\mathbf{m}_{hk}, \mathbf{m}_{hk}^{\pm}, \overline{\mathbf{m}}_{hk} &\to \mathbf{m} && \text{in } \mathbf{L}^2(\omega_T),\\
\mathbf{H}_{hk}, \mathbf{H}_{hk}^{\pm}, \overline{\mathbf{H}}_{hk} &\rightharpoonup \mathbf{H} && \text{in } \mathbf{L}^2(\Omega_T),\\
\mathbf{E}_{hk}, \mathbf{E}_{hk}^{\pm}, \overline{\mathbf{E}}_{hk} &\rightharpoonup \mathbf{E} && \text{in } \mathbf{L}^2(\Omega_T),\\
\mathbf{v}_{hk}^{-} &\rightharpoonup \mathbf{v} && \text{in } \mathbf{L}^2(\omega_T).
\end{aligned}$$

The proof of Theorem 5.2 for Algorithm 4.1 then completely follows the lines of the one for Algorithm 4.2.

6. Numerical examples. We study the standard μ-mag benchmark problem[1] number 4, using Algorithm 4.1 and Algorithm 4.2. Here, the effective field consists of the magnetic field $\mathbf{H}$ from the Maxwell equations and some constant external field $\mathbf{H}_{ext}$, i.e., $\pi(\mathbf{m}_h^j) = \mathbf{H}_{ext}$ for all $j = 1, \dots, N$. This problem has been solved previously using the midpoint scheme in [6], and we also use those results for comparison.

Despite the fact that the system (4.1) in Algorithm 4.1 is linear, for computational reasons it is preferable to solve LLG and the Maxwell equations separately. After decoupling, the corresponding linear systems can be solved using dedicated linear solvers. This leads to a considerable improvement in computational performance; cf. [7]. In order to decouple the respective equations in (4.1), we employ a simple block Gauss-Seidel algorithm. For simplicity we set $\sigma \equiv 0$, $\mathbf{J} \equiv \mathbf{0}$. Assuming the solution $\mathbf{v}_h^{j-1}$, $\mathbf{H}_h^j$, $\mathbf{E}_h^j$ is known for a fixed time level j, we set $\mathbf{G}_h^0 = \mathbf{H}_h^j$, $\mathbf{F}_h^0 = \mathbf{E}_h^j$, and $\mathbf{w}_h^0 = \mathbf{v}_h^{j-1}$ and iterate the following problem over ℓ:

[1] see the Micromagnetic Modeling Activity Group
http://www.ctcms.nist.gov/~rdm/mumag.org.html

ETNA
Kent State University
http://etna.math.kent.edu

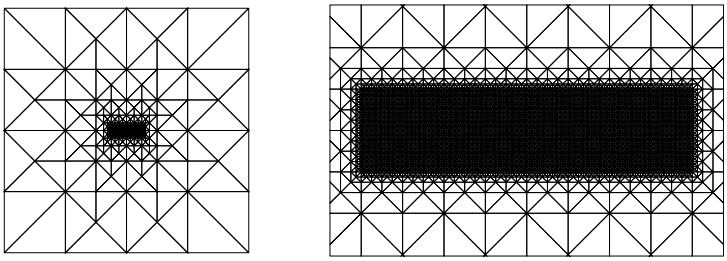

FIG. 6.1. *Mesh for the domain Ω at $x_3 = 0$ (left) and zoom at the mesh for the domain ω at $x_3 = 0$ (right).*

Find $\mathbf{w}_h^\ell, \mathbf{F}_h^\ell, \mathbf{G}_h^\ell \in \mathcal{K}_{\mathbf{m}_h^j} \times \mathcal{X}_h \times \mathcal{Y}_h$ such that for all $\boldsymbol{\phi}_h, \boldsymbol{\psi}_h, \boldsymbol{\zeta}_h \in \mathcal{K}_{\mathbf{m}_h^j} \times \mathcal{X}_h \times \mathcal{Y}_h$, we have

$$\begin{aligned}\alpha\langle \mathbf{w}_h^\ell, \boldsymbol{\phi}_h\rangle_\omega + \langle \mathbf{m}_h^j \times \mathbf{w}_h^j, \boldsymbol{\phi}_h\rangle_\omega &= -C_e\langle \nabla(\mathbf{m}_h^j + \theta k \mathbf{w}_h^\ell), \nabla\boldsymbol{\phi}_h\rangle_\omega \\ &\quad + \langle \mathbf{G}_h^{\ell-1} + \mathbf{H}_{ext}, \boldsymbol{\phi}_h\rangle_\omega,\end{aligned} \tag{6.1a}$$

$$\varepsilon_0 \frac{2}{k}\langle \mathbf{F}_h^\ell, \boldsymbol{\psi}_h\rangle_\Omega - \langle \mathbf{G}_h^\ell, \nabla\times\boldsymbol{\psi}_h\rangle_\Omega = \varepsilon_0\frac{2}{k}\langle \mathbf{E}_h^j, \boldsymbol{\psi}_h\rangle_\Omega, \tag{6.1b}$$

$$\mu_0 \frac{2}{k}\langle \mathbf{G}_h^\ell, \boldsymbol{\zeta}_h\rangle_\Omega + \langle \nabla\times\mathbf{F}_h^\ell, \boldsymbol{\zeta}_h\rangle_\Omega = \mu_0\frac{2}{k}\langle \mathbf{H}_h^j, \boldsymbol{\zeta}_h\rangle_\Omega - \mu_0\langle \mathbf{w}_h^\ell, \boldsymbol{\zeta}_h\rangle_\omega, \tag{6.1c}$$

until $\|\mathbf{w}_h^\ell - \mathbf{w}_h^{\ell-1}\|_\infty + \|\mathbf{G}_h^\ell - \mathbf{G}_h^{\ell-1}\|_\infty + \|\mathbf{F}_h^\ell - \mathbf{F}_h^{\ell-1}\|_\infty < TOL$. In this setting, $\mathbf{F}_h^\ell$ is an approximation of $\mathbf{E}_h^{j+1/2}$ and $\mathbf{G}_h^\ell$ is an approximation of $\mathbf{H}_h^{j+1/2}$, respectively. Therefore, we have

$$\frac{2}{k}(\mathbf{F}_h^\ell - \mathbf{E}_h^j) \approx \frac{2}{k}(\mathbf{E}_h^{j+1/2} - \mathbf{E}_h^j) = \frac{\mathbf{E}_h^{j+1} - \mathbf{E}_h^j}{k} = d_t\mathbf{E}_h^{j+1}.$$

Analogous treatment of the $\mathbf{H}_h^{j+1/2}$-term thus motivates the above algorithm. We obtain the solution on the time level $j+1$ as $\mathbf{v}_h^j = \mathbf{w}_h^\ell$, $\mathbf{H}_h^{j+1} = 2\mathbf{G}_h^\ell - \mathbf{H}_h^j$, $\mathbf{E}_h^{j+1} = 2\mathbf{F}_h^\ell - \mathbf{E}_h^j$. The linear system (6.1a) is solved using a direct solver, where the constraint on the space $\mathcal{K}_{\mathbf{m}_h^j}$ is realized via a Lagrange multiplier; see [25]. For the solution of the linear system (6.1b)–(6.1c) we employ a multigrid preconditioned Uzawa algorithm from [7].

The physical parameters that were used for the computation were $\mu_0 = 1.25667 \times 10^{-6}$, $\varepsilon_0 = 0.88422 \times 10^{-11}$, $A = 1.3 \times 10^{-11}$, $M_s = 8 \times 10^5$, $\gamma = 2.211 \times 10^5$, $\alpha = 0.02$, $\mathbf{H}_{ext} = (\mu_0 M_s)^{-1}(-24.6, 4.3, 0)$, and $C_e = 2A(\mu_0 M_s^2)^{-1}$. Here, γ denotes the gyromagnetic ratio, and M_s is the so-called saturation magnetization; see, e.g., [16]. We set $\theta = 1$ in both Algorithms 4.1 and 4.2. The ferromagnetic domain $\omega = 0.5 \times 0.125 \times 0.003$ $(\mu\mathrm{m})$ is uniformly partitioned into cubes with dimensions of $(3.90625 \times 3.90625 \times 3)(n\mathrm{m})$, each cube consisting of six tetrahedra. The Maxwell equations are solved on the domain $\Omega = (4 \times 4 \times 3.072)$ $(\mu\mathrm{m})$. The finite element mesh for the domain Ω is constructed by gradual refinement towards the ferromagnetic domain ω, see Figure 6.1. We take a uniform time step $k = 0.05$ which is two times larger than the time step required for the midpoint scheme [6]. Note that the scheme admits time steps up to $k = 1$, the smaller time step has been chosen to attain the desired accuracy.

The initial condition $\mathbf{m}_0$ for the magnetization is an equilibrium "S-state", see Figure 6.2, which is computed from a long-time simulation as in [6, 7]. The initial condition $\mathbf{H}_0$ is obtained from the magnetostatic approximation of the Maxwell equations with and $\mathbf{E}_0 = \mathbf{0}$; for details see [6]. In Figure 6.3 we plot the evolution of the average components m_1 and m_2 of the magnetization for Algorithm 4.1 and Algorithm 4.2. For comparison, we also present the results computed with the midpoint scheme from [6] with time step $k = 0.02$.

ETNA
Kent State University
http://etna.math.kent.edu

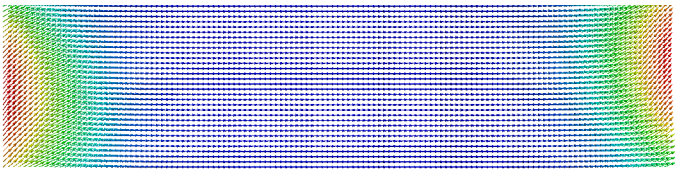

FIG. 6.2. *Initial condition* $\mathbf{m}^0$.

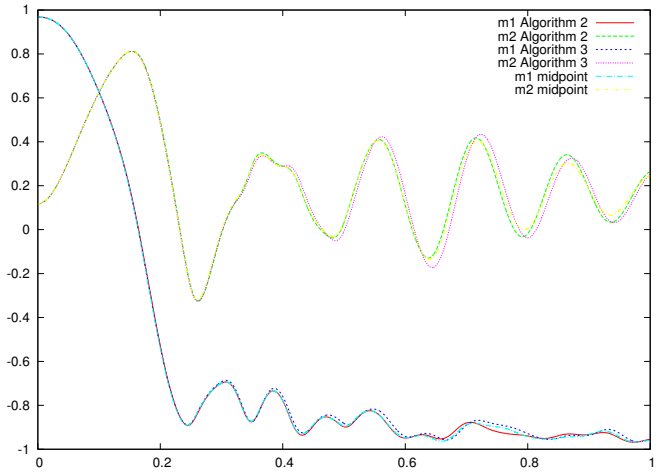

FIG. 6.3. *Evolution of* $|\omega|^{-1}\int_\omega m_1$ *and* $|\omega|^{-1}\int_\omega m_2$, *where* m_j *denotes the* j*-th component of the computed magnetization* $\mathbf{m}:\omega\to\mathbb{R}^3$. *Algorithm 2 refers to Algorithm 4.1 and Algorithm 3 to Algorithm 4.2.*

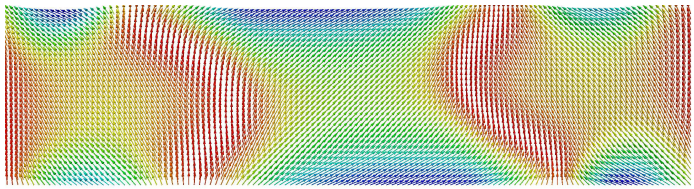

FIG. 6.4. *Algorithm 4.1: solution at* $|\omega|^{-1}\int_\omega m_1(t)=0$.

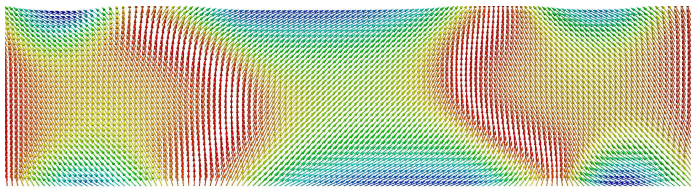

FIG. 6.5. *Midpoint scheme from [6, 7]: solution at* $|\omega|^{-1}\int_\omega m_1=0$.

We also show a snapshot of the magnetization for Algorithm 4.1 and the midpoint scheme at times when $|\omega|^{-1}\int_\omega m_1(t)=0$ in Figures 6.4 and 6.5, respectively. We conclude that the results for both algorithms are in good agreement with those computed with the midpoint scheme.

ETNA
Kent State University
http://etna.math.kent.edu

Acknowledgements. The authors acknowledge financial support though the WWTF project MA09-029 and the FWF project P21732.

REFERENCES

[1] C. ABERT, G. HRKAC, M. PAGE, D. PRAETORIUS, M. RUGGERI, AND D. SÜSS, *Spin-polarized transport in ferromagnetic multilayers: an unconditionally convergent FEM integrator*, Comput. Math. Appl., 68 (2014), pp. 639–654.

[2] F. ALOUGES, *A new finite element scheme for Landau-Lifchitz equations*, Discrete Contin. Dyn. Syst. Ser. S, 1 (2008), pp. 187–196.

[3] F. ALOUGES, E. KRITSIKIS, AND J. TOUSSAINT, *A convergent finite element approximation for Landau-Lifshitz-Gilbert equation*, Phys. B, 407 (2012), pp. 1345–1349.

[4] ———, *A convergent and precise finite element scheme for Landau-Lifschitz-Gilbert equation*, Numer. Math., 128 (2014), pp. 407–430.

[5] F. ALOUGES AND A. SOYEUR, *On global weak solutions for Landau-Lifshitz equations: existence and nonuniqueness*, Nonlinear Anal., 18 (1992), pp. 1071–1084.

[6] Ľ. BAŇAS, *An efficient multigrid preconditioner for Maxwell's equations in micromagnetism*, Math. Comput. Simulation, 80 (2010), pp. 1657–1663.

[7] Ľ. BAŇAS, S. BARTELS, AND A. PROHL, *A convergent implicit finite element discretization of the Maxwell-Landau-Lifshitz-Gilbert equation*, SIAM J. Numer. Anal., 46 (2008), pp. 1399–1422.

[8] Ľ. BAŇAS, Z. BRZEŹNIAK, AND A. PROHL, *Computational studies for the stochastic Landau-Lifshitz-Gilbert equation*, SIAM J. Sci. Comput., 35 (2013), pp. B62–B81.

[9] Ľ. BAŇAS, M. PAGE, AND D. PRAETORIUS, *A convergent linear finite element scheme for the Maxwell-Landau-Lifshitz-Gilbert equation*, ASC Report 09/2013, Institute for Analysis and Scientific Computing, Vienna University of Technology, 2013.

[10] Ľ. BAŇAS, M. PAGE, D. PRAETORIUS, AND J. ROCHAT, *On the Landau-Lifshitz-Gilbert equations with magnetostriction*, IMA J. Numer. Anal., 34 (2014), pp. 1361–1385.

[11] S. BARTELS, *Stability and convergence of finite-element approximation schemes for harmonic maps*, SIAM J. Numer. Anal., 43 (2005), pp. 220–238.

[12] ———, *Projection-free approximation of geometrically constrained partial differential equations*, Math. Comp., accepted, 2015.

[13] S. BARTELS, J. KO, AND A. PROHL, *Numerical analysis of an explicit approximation scheme for the Landau-Lifshitz-Gilbert equation*, Math. Comp., 77 (2008), pp. 773–788.

[14] S. BARTELS AND A. PROHL, *Convergence of an implicit finite element method for the Landau-Lifshitz-Gilbert equation*, SIAM J. Numer. Anal., 44 (2006), pp. 1405–1419.

[15] S. BRENNER AND L. SCOTT, *The Mathematical Theory of Finite Element Methods*, 2nd ed., Springer, New York, 2002.

[16] F. BRUCKNER, D. SUESS, M. FEISCHL, T, FÜHRER, P. GOLDENITS, M. PAGE, D. PRAETORIUS, AND M. RUGGERI, *Multiscale modeling in micromagnetics: well-posedness and numerical integration*, Math. Models Methods Appl. Sci., 24 (2014), pp. 2627–2662.

[17] F. BRUCKNER, C. VOGLER, B. BERGMAIR, T. HUBER, M. FUGER, D. SUESS, M. FEISCHL, T. FÜHRER, M. PAGE, AND D. PRAETORIUS, *Combining micromagnetism and magnetostatic Maxwell equations for multiscale magnetic simulation*, J. Magn. Magn. Mater., 343 (2013), pp. 163–168.

[18] G. CARBOU AND P. FABRIE, *Time average in micromagnetism*, J. Differential Equations, 147 (1998), pp. 383–409.

[19] I. CIMRAK, *A survey on the numerics and computations for the Landau-Lifshitz equation of micromagnetism*, Arch. Comput. Methods Eng., 15 (2008), pp. 277–309.

[20] M. D'AQUINO, C. SERPICO, AND G. MIANO, *Geometrical integration of Landau-Lifshitz-Gilbert equation based on the mid-point rule*, J. Comput. Phys., 209 (2005), pp. 730–753.

[21] J. ELSTRODT, *Maß- und Integrationstheorie*, 6th ed., Springer, Heidelberg, 2009.

[22] C.J. GARCÍA-CERVERA, *Numerical micromagnetics: a review*, Bol. Soc. Esp. Mat. Apl. CẽMA, 39 (2007), pp. 103–135.

[23] G. HRKAC, *Combining Eddy-Current and Micromagnetic Simulations with Finite-Element method*, PhD Thesis, Institute for Solid State Phys., Vienna University of Technology, 2005.

[24] P. GOLDENITS, *Konvergente numerische Integration der Landau-Lifshitz-Gilbert Gleichung*, PhD Thesis, Institute for Analysis and Scientific Computing, Vienna University of Technology, 2012.

[25] P. GOLDENITS, G. HRKAC, M. MAYR, D. PRAETORIUS, AND D. SUESS, *An effective integrator for the Landau-Lifshitz-Gilbert equation*, Proceedings of Mathmod 2012 Conference, I. Troch and F. Breitenecker, eds., International Federation of Automatic Control, Vienna, 2014, pp. 493–497.

[26] P. GOLDENITS, D. PRAETORIUS, AND D. SUESS, *Convergent geometric integrator for the Landau-Lifshitz-Gilbert equation in micromagnetics*, Proc. Appl. Math. Mech., 11 (2011), pp. 775–776.

ETNA
Kent State University
http://etna.math.kent.edu

[27] A. HUBERT AND R. SCHÄFER, *Magnetic Domains. The Analysis of Magnetic Microstructures*, Springer, Heidelberg, 1998.
[28] K. LE, M. PAGE, D. PRAETORIUS, AND T. TRAN, *On a decoupled linear FEM integrator for eddy-current-LLG*, Appl. Anal., in press, 2014, doi: 10.1080/00036811.2014.916401.
[29] K. LE AND T. TRAN, *A convergent finite element approximation for the quasi-static Maxwell-Landau-Lifshitz-Gilbert equations*, Comput. Math. Appl., 66 (2013), pp. 1389–1402.
[30] M. KRUZIK AND A. PROHL, *Recent developments in the modeling, analysis, and numerics of ferromagnetism*, SIAM Rev., 48 (2006), pp. 439–483.
[31] P. B. MONK, *Finite Element Methods for Maxwell's Equations*, Oxford University Press, Oxford, 2003.
[32] P. B. MONK AND O. VACUS, *Accurate discretization of a non-linear micromagnetic problem*, Comput. Methods Appl. Mech. Engrg., 190 (2001), pp. 5243–5269.
[33] M. PAGE, *On Dynamical Micromagnetism*, PhD Thesis, Institute for Analysis and Scientific Computing, Vienna University of Technology, 2013.
[34] A. PROHL, *Computational Micromagnetism*, B. G. Teubner, Stuttgart, 2001.
[35] J. RIVAS, J.M. ZAMARRO, E. MARTÍN, AND C. PEREIRA, *Simple approximation for magnetization curves and hysteresis loops*, IEEE Trans. Magn., 17 (1981), pp. 1498–1502.
[36] R. VERFÜRTH, *A Review of A Posteriori Error Estimation and Adaptive Mesh-Refinement Techniques*, Wiley-Teubner, Stuttgart, 1996.
[37] A. VISINTIN, *On Landau-Lifshitz' equations for ferromagnetism*, Japan J. Appl. Math., 2 (1985), pp. 69–84.